EPSC Abstracts
Vol. 10, EPSC2015-130, 2015
European Planetary Science Congress 2015

Critical components of Venus Lower and Upper atmospheres with FirefOx and Venus Neutron Spectrometer (VeNuS)

N. R. Izenberg, S. J. Papadakis, A. H. Monica, D. M. Deglau, D. J. Lawrence, P. N. Peplowski, The Johns Hopkins University Applied Physics Laboratory, 11100 Johns Hopkins Road, Laurel, MD 20723, USA (noam.izenberg@jhuapl.edu / Fax: +1-443-778-6670)

Abstract

We present two instrument concepts for understanding critical aspects of Venus' upper and lower atmosphere. FirefOx is an oxygen fugacity sensor for the lower atmosphere, and The Venus Nuclear Spectrometer (VeNuS) studies composition and volcanic activity signals in the upper atmosphere.

1. FirefOx

Oxygen is a trace gas in the lower atmosphere of Venus, controlled by the CO-CO_2 chemical equilibrium. At mean planetary radius, with temperature of approximately 740 K, fO_2 is calculated to be ~$10^{-21.5}$ bars [1,2]. Lower actual CO values at the surface (i.e. below the 20 ppm measured at 22 km), oxygen fugacity would be higher. Observational and theoretical constraints suggest a CO abundance of 3-20 ppm at the surface of Venus [1], thus a plausible range of oxygen fugacity would be ~ 10^{-20} bars to ~10^{-24} bars.

Direct measurement of fO_2 would both improve understanding of the carbon gas chemistry in the lower atmosphere of Venus. This might change predicted mineral stability regimes, and thus mineral phases present presented at the surface of Venus [2]. Direct measurement of the partial pressure of oxygen would provide robust constraints on gas chemistry and surface mineral stability, and confirmation of carbon gas measurements obtained by other methods.

FirefOx is a metal/metal oxide oxygen fugacity sensor to be mounted on the outside of a Venus descent probe or lander, with electronics to be housed inside a thermally controlled environment. It is a simple, low power and cost sensor derived from common industrial and off-the-shelf ceramic oxygen sensors, with the express purpose of determining the partial pressure of oxygen in the lowest scale heights of the Venus atmosphere, and especially the lowest hundreds of meters and the surface-atmosphere interface, where the atmosphere and surface move to thermodynamic equilibrium.

The primary sensor capability is the detection of the partial pressure of oxygen gas (fO2) in the near-surface environment of Venus, so the sensor must operate in the 710-740K temperature range and at up to 95-bar pressure (predominantly CO2) for sufficient time to obtain a precise, accurate measurement. The baseline sensor objective is survival for at least two hours at Venus surface conditions, and produce accurate measurements (fO2 to 0.5 +/- 0.5x10-24 within the range of 10-18 to 10-24) at a temperature range between 710 and 740K. Mean planetary elevation has a temperature near 735 K, and the operational temperature range covers a range of potential landing elevations. FirefOx requirements are low (~100-200 grams, milliwatt power, several kilobytes total science data), while its potential science return is high.

The FirefOx oxygen sensor is a solid-state, solid electrolyte oxygen concentration cell (henceforth called a ceramic oxygen sensor). Ceramic oxygen sensors have been used to measure oxygen fugacity in hot gases for nearly 50 years [3]. The basic principle relies on a reference material of a known fO_2, a solid electrolyte, and a sample atmosphere or material. The fO_2 differential between the known and unknown materials causes a diffusion of oxygen through the electrolyte, resulting in a small, measurable voltage.

A simple COS fO_2 sensor should follow the Nernst equation [cf. 4,5], and is thus a primary sensor (in other words, one that should not actually need calibration, but whose output is fundamentally related to the inputs). The Nernst equation directly relates the potential generated by the diffusing

oxygen atoms through the sensor to the fO_2 via a relationship similar to

$$E = RT/4F \ln(P_{O2}/P_{refO2}) \quad (1)$$

Where E is the open circuit potential across the sensor electrolyte (directly measured by the sensor), R is the universal gas constant, T is the temperature, F is the Faraday constant, P_{refO2} is the reference oxygen pressure on one side of the electrolyte (metal oxide), and P_{O2} is the unknown oxygen pressure of the outside environment [5]

2. VeNuS

Nuclear (gamma-ray and neutron) spectroscopy is a proven technique for measuring the elemental composition of planetary surfaces, including Venus [6]. The technique has also been used to characterize the composition and time variability of planetary atmospheres [7-9]. An orbital Venus Nuclear Spectrometer would address important questions regarding key constituents and events in the Venus upper atmosphere [10].

2.1 Lightning Monitoring:

Lightning is an important dynamical process in atmospheres, and determining the frequency, time-, and spatial-dependence of lightning on Venus is an important goal. Earth-orbiting gamma-ray observatories have detected and mapped terrestrial gamma-ray flashes from upward lightning events across the surface of the Earth [e.g. 11]. A gamma-ray detector on a low-altitude (<2 Venus radii) orbiter would likewise provide real-time monitoring to search for similar lightning-induced gamma rays at Venus [12].

2.2 Atmospheric Composition:

Neutron spectroscopy is sensitive to the abundances of neutron moderating (e.g. H, C, N, O) and absorbing (e.g. Ar, S, Cl, H) elements. A MESSENGER- or Lunar Prospector heritage Neutron Spectrometer on a low-altitude Venus-orbiting spacecraft can be used to derive the bulk abundances of neutron moderating and absorbing elements within the atmosphere at altitudes of 65-80 km. This capability supports two measurements:

1) Derivation of the nitrogen content of the upper atmosphere. Despite being the second-most-abundant compound in Venus' atmosphere, the volume mixing ratio for N_2 is unknown by ±23% [13]. Knowledge of the N content of Venus' atmosphere is crucial for understanding the divergent evolutions of the atmospheres of Venus, Earth, and Mars [14]. Neutron fluxes measured by VeNuS, combined with constraints on the atmospheric composition from prior in-situ experiments [e.g. 13] will provide a precise (<5% uncertainty) determination of the N content of the upper atmosphere.

2) Monitoring volcanic gas concentrations. There is tantalizing evidence for ongoing volcanic activity on the surface of Venus, including from long-term monitoring (1978-1996, 2006-2012) of the SO_2 content of Venus' atmosphere [15-17]. That data shows variability that may be associated with periodic eruptive events that injecting volcanic gas into the upper atmosphere. VeNuS would provide a time-series measurement that is highly sensitive to the bulk concentration of thermal neutron absorbing elements (Ar, S, Cl, and H), which are all expected to be byproducts of volcanic activity. This technique provide time-series measurements of key elements associated with volcanic activity as injected into the upper atmosphere, a crucial constraint on the frequency of present-day volcanic activity on Venus.

References

[1] Fegley, B. Jr. et al., (1997), *Icarus*, *125*(2), 416-439.

[2] Fegley, B. Jr. and Trieman, A. H. (1992), *Venus and Mars: AGU Monogrpah 66*, 7-71.

[3] Nenov, T., and Yordanov, S. P., (1996), CRC Press.

[4] Arculus, R. J., and Delano, J. W., (1981), *Geo. et Cosmo. Acta* 45, 899-913.

[5] Van Setten, E. et al., (2002), *Rev. Sci. Inst.*, *73*, 156-161.

[6] Surkov, Y.A. et al. (1987), JGR 92, E537-540.

[7] Feldman, W.C. et al. (2003), JGR 108, E95103.

[8] Sprague, A.L. et al. (2004), Science 306, 1364-1367.

[9] Prettyman, T.H. et al. (2004), JGR 109, E05001.

[10] VEXAG GOI (2014)

[11] Fishman, G. J et al. (1994), Science 264, 5163.

[12] Lorenz, R.D. and Lawrence, D.J. (2015) PSS (in re-view).

[13] von Zahn, U. et al. (1983), in Venus (U. AZ. Press), 299-430.

[14] Lecuyer et al. (2000), EPSL 181, 33-40.

[15] Esposito, L.W. et al. (1984), Science 223, 1072-1074.

[16] Esposito, L.W. et al. (1988), JGR 93, 5267-5276.

[17] Marcq, E. et al. (2013), Nat. Geosci. 6, 25-28.

EPSC Abstracts
Vol. 10, EPSC2015-185, 2015
European Planetary Science Congress 2015

The SuperCam Instrument for the Mars2020 Rover

S. Maurice[1], R.C. Wiens[2], S. Le Mouélic[3], R. Anderson[4], O. Beyssac[5], L. Bonal[6], S. Clegg[2], L. DeFlores[7], G. Dromart[8], W. Fischer[9], O. Forni[1], O. Gasnault[1], J. Grotzinger[9], J. Johnson[10], J. Martinez-Frias[11], N. Mangold[3], S. McLennan[12], F. Montmessin[13], F. Rull[15], S. Sharma[14], and the SuperCam** team. [1]IRAP, Toulouse, France (sylvestre.maurice@irap.omp.eu); [2]LANL, Los Alamos; [3]LPGN, Nantes; [4]USGS, Flagstaff, AZ; [5]IMPMC, Paris; [6]IPAG, Grenoble; [7]JPL, Pasadena; [8]LGLTPE, Lyon; [9]Caltech, Pasadena; [10]APL/JHU, Laurel; [11]CSIC-UCM, Madrid; [12]Stony Brook Univ.; [13]LATMOS, Guyancourt; [14]HIGP, Hawai'I; [15]UVA-CSIC, Valladolid.

1. Introduction

Micro-scale characterization of the mineralogy and elemental chemistry of the Martian surface, along with the search for organic materials, are fundamental investigations that lay the groundwork for all types of Mars geochemistry and astrobiology investigations. SuperCam, being developed for the Mars 2020 rover, is a suite of four co-aligned instruments that remotely provide these critical observations via Laser Induced Breakdown Spectroscopy (LIBS), Raman spectroscopy, time-resolved fluorescence (TRF), visible and near-infrared spectroscopy (VISIR), and high resolution color remote micro-imaging (RMI) (Fig. 1). The LIBS, VIS, and RMI capabilities rely heavily on heritage from the ChemCam instrument on MSL [e.g. 1]. Information on the LIBS, Raman, and TRF investigations and their implementation can be found in [2]. VISIR is described in [3] and RMI in [4].

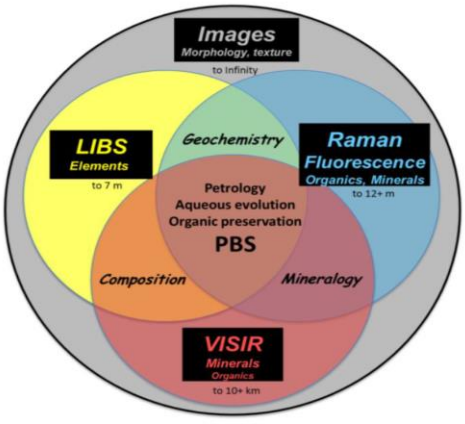

Fig. 1. SuperCam investigations contributing to the detection of Potential Biosignatures (PBS).

We focus here on the overall science objectives and their relationship with the mission goals, on the characteristic scale of each investigation, and on the implementation of observation modes to account for the versatility of the instrument.

2. Science objectives

The Science Definition Team (SDT [5]) defined four separate goals for the 2020 mission to assess whether life developed on Mars and to assemble a returnable cache of samples. Fig. 2 shows how SuperCam science objectives map with the mission goals.

1. *Rock Identification*: Mineral, chemical and textural characterization of rocks will help to determine the geological diversity, identify key processes relevant to the aqueous history, and document the context of the sample cache.
2. *Sedimentology and Stratigraphy*: Characterization of the texture and composition of the sedimentary structures will provide strong constraints for the aqueous processes as well as potential habitability.
3. *Organics and Bio-signatures*: SuperCam will remotely analyze astrobiologically relevant materials, determining the best area for contact science and caching.

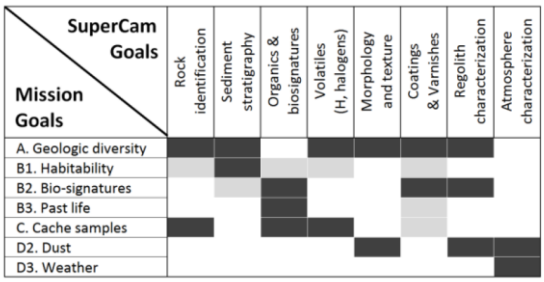

Fig. 2. Science goals and their relationship with mission objectives.

4. *Volatiles*: SuperCam will constrain the aqueous processes involving volatiles and provide data on volatile content for the documentation of cached material.
5. *Context Morphology and Texture*: High resolution color images will provide detailed information on dust cover, target morphology and texture.
6. *Coatings and Varnishes*: Analyses of coatings will allow the identification of late-stage weathering and its relationship (if any) to biological activity.

7. *Regolith Characterization*: SuperCam will address soil diversity and characterize its potential for biosignature preservation.
8. *Atmospheric Characterization*: Atmospheric molecules, water ice, and dust characteristics will address the radiative balance of the atmosphere, and will prepare for human exploration.

3. Remote Sensing and Sampling Scales.

SuperCam will make thousands of measurements at remote distances, within and beyond the arm workspace. Each co-boresighted investigation has its range of distances to target, from 2 m to 7 m for LIBS, up to 12 m for Raman and TRF, up to the horizon for VISIR and RMI, with different sampling scales. The LIBS analysis area is 300 – 600 µm in diameter. Single laser shots probe a few µm in depth, whereas hundreds of laser shots can probe up to ~500 µm in rocks. The Raman, TRF, and VISIR analysis footprints are similar, at 0.67 mrad (1.3 mm at 2 m distance). The imaging field of view is 20 mrad (pixel FOV of 20 µrad, i.e. 40 µm at 2 m).

The SDT recommended six threshold measurements including context 1) imaging and 2) mineralogy, fine-scale 3) imaging, 4) mineralogy, and 5) elemental chemistry, and 6) organic detection. SuperCam clearly meets the scale requirements (1, 2) of the context measurements, though SuperCam is not the primary context camera (Mastcam-Z fills this role). With "scan mode", SuperCam can survey an area rapidly. SuperCam provides organic detection (6) on a broad survey scale using remote Raman, fluorescence, and VISIR spectroscopy. SuperCam also meets or approaches the SDT resolution criteria at close range (3, 4, 5). We expect arm-mounted instruments (PiXL, SHERLOC) to fulfil the fine-scale requirements.

4. Observation modes

To account for the diversity of situations, several modes of investigations are being defined (Fig. 3).

 Survey raster, a combination of single points to study lateral heterogeneity and chemostratigraphy. This involves the full suite of investigations within 7 m; Raman up to 12 m, and VISIR beyond.
 Depth profile, a unique capability of LIBS to probe the first 10 – 500 microns below the surface.

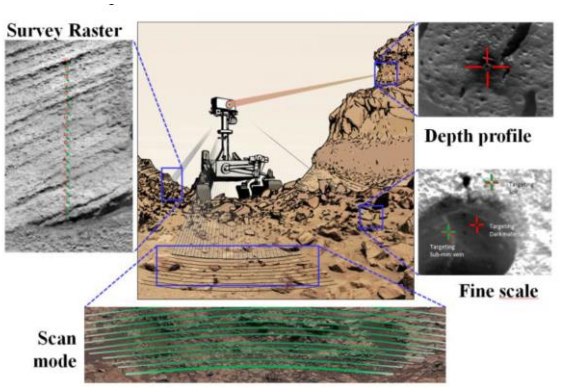

Fig. 3: Observation modes of SuperCam.

 Scan mode, 30° exploration in azimuth at close range (Raman + VISIR) and longer range (VISIR). While the mast is rotated at its slowest speed, Raman and/or VISIR spectra are acquired continuously.
 Fine scale Mode, targeted pointing at < 7 m for full chemistry and mineralogy investigations. Using JPL onboard software, AEGIS [6], laser shots can be auto-targeted at very small (e.g., mm or sub-mm) objects of interests (veins, nodules, laminae, etc.)

"Scan" and "raster" modes will be predominantly used when approaching a region-of-interest. "Fine scale" and "depth profile" modes will be used to select and document sample caching. A typical Sol on Mars might contain 11 LIBS, 8 Raman (including at least 1 time-resolved fluorescence), 16 VISIR points, and 10 images.

5. Management

SuperCam is a multi-national instrument. The US contribution is funded by NASA. R. Wiens at LANL is the instrument PI. The French contribution is funded by CNES. S. Maurice at IRAP is the deputy-PI. Spain under the leadership of F. Rull at UVA is responsible of the instrument calibration targets.
**Other collaborators of the SuperCam team are: V. Sautter, E. Lewin, E. Cloutis, F. Poulet, S. Bernard, T. McConnochie, N. Lanza, H. Newsom, A. Ollila, R. Leveille, J. Lasue, N. Melikechi, P-Y Meslin, A. Misra, O. Grasset, M.Angel, T. Fouchet, P. Beck,P. Sobron, N. Bridges, B. Bousquet, C. Fabre, P. Pinet, K. Benzarara, G. Montagnac.

References: [1] Anderson R. et al. (2015), *Icarus, 249, 2-21*. [2] Clegg S. M. et al. (2015) *LPSC XLVI*, #2781. [3] Fouchet T. et al. (2015) *LPSC XLVI*, #1736. [4] Gasnault O. et al. (2015*) LPSC XLVI*, #2990. [5] Mustard J. et al. (2013): Report of the Mars 2020 Science Def. Team. [6] Estlin T. et al. (2013), AGU Meeting, abstract #P51G-1801.

EPSC Abstracts
Vol. 10, EPSC2015-212, 2015
European Planetary Science Congress 2015

Ground-based VLBI observations of orbiters and landers

G. Cimò (1), D.A. Duev (1), G. Molera Calvés (1,2), S. V. Pogrebenko (1), T. Bocanegra Bahamon (1,3,4) and L. I. Gurvits (1,3)

(1) Joint Institute for VLBI − European Research Infrastructure Consortium, The Netherlands (cimo@jive.nu / Fax: +31-521-596539), (2) Metsähovi Radio Observatory, Finland, (3) Delft University of Technology, The Netherlands, (4) Shanghai Astronomical Observatory, China

Abstract

Phase referencing near-field VLBI observations and radial Doppler measurements of spacecraft provide ultra-precise estimates of spacecraft state vectors. These measurements can be used for a variety of scientific applications, both fundamental and applied, including planetary science, improvement of ephemerides, ultra-precise celestial mechanics of planetary systems, gravimetry, spacecraft orbit determination, and fundamental physics.

Precise determination of the lateral position of spacecraft on the celestial sphere is the main deliverable of the Planetary Radio Interferometry and Doppler Experiment (PRIDE). This technique is complementary to radio science experiments and addresses those areas of spacecraft mission science objectives that require accurate estimation of spacecraft state vector.

Applications of Near field VLBI

The scientific applications of the Planetary Radio Interferometry and Doppler Experiment are based on two observable quantities: the radial range rate (Doppler shift of the service communication system carrier signal) and the lateral (transverse) celestial position of the spacecraft with respect to the International Celestial Reference Frame (ICRF). The measurements of the spacecraft differential lateral position relative to ICRF are performed by VLBI observations of spacecraft and background extragalactic radio sources with accuracy of tens of μas (1-σ RMS) over integration time of $60 - 1000$ s[2]. The direct measurables of PRIDE are shown in Figure 1.

The PRIDE experiment is a direct descendant of legacy VLBI experiments with the VEGA [1], Huygens [5], IKAROS [7] and other planetary missions.

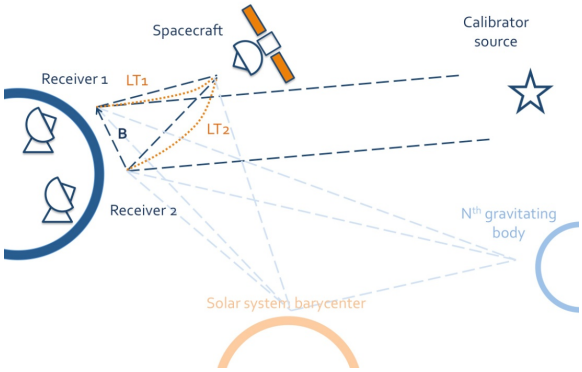

Figure 1: Geometry of a PRIDE experiment.

The use of the Very Long Baseline Interferometry for supporting of planetary missions was developed more than thirty years ago and has been used in missions requiring ultimate accuracy of a posteriori trajectory determination [8]. In the recent years, Jones [9] has observed the Cassini spacecraft using the Very Long Baseline Array (VLBA) to improve Saturn ephemeris.

The PRIDE team carried out a number of experiments to develop and improve VLBI and Doppler measurements of spacecraft and to study their scientific applications. ESA's Venus Express (VEX) and Mars Express (MEX) has been extensively targeted by PRIDE for studying the solar wind by observing the effects of intervening ionized plasmas on the spacecraft signal [3]. Radio occultation experiments of both Venus Express and Mars Express have performed to derive vertical density, pressure and temperature profiles of planetary atmospheres. In the case of MEX, a number of observations were carried out during the Phobos flyby on December 2013. Both Doppler and VLBI measurements can be used to improve the determination of the Phobos' gravity field derived so far from radioscience only [4]. The radioscience and VLBI data are complementary as the precise former data will be

complemented by constraints from the VLBI measurements. Finally, we will present results of the VLBI tracking of the ESA's space astrometry mission, Gaia, which has been targeted by the PRIDE team as a test experiment to improve the VLBI algorithm and to explore the possibility to track Gaia in order to enhance significantly the mission science output, especially in the areas of parallaxes and identification of Solar System's small bodies where accuracy of the order of one milliarcsecond is required.

PRIDE is an experiment with zero impact on the science payload mass, and it offers a high degree of synergy with the typical on-board instrumentation. Near field VLBI can complement the scientific suite of any future missions with transmitting orbiters and/or landers. The flexibility of PRIDE and its many scientific outcomes for the minimal requirements have contributed to make PRIDE one of the selected experiments for JUICE (JUpiter ICy moons Explorer), the next ESA's L-class mission.

Acknowledgments

The authors acknowledge the EC FP7 project ESPaCE (grant agreement 263466). T. Bocanegra Bahamon acknowledges the NWO-ShAO agreement on collaboration in VLBI.

References

[1] Preston, R., et al. 1986, Science 231, 4744, 1414

[2] D. A. Duev, G. Molera Calvés, S. V. Pogrebenko, L. I. Gurvits, G. Cimò and T. Bocanegra Bahamon: Spacecraft VLBI and Doppler tracking: algorithms and implementation, Astronomy & Astrophysics, Vol. 541, 2012.

[3] Molera Calvés G., Cimò, G., Pogrebenko, S.V. & et al., 2014, A&A 564, A4

[4] Rosenblatt et al, in preparation.

[5] Jean-Pierre Lebreton et al: An overview of the descent and landing of the Huygens probe on Titan, Nature 438, 2005.

[6] Fridman P.A., L. Gurvits and S. Pogrebenko: The SKA as a Direct-to-Earth Data Acquisition Facility for Deep Space Science Missions, SKA2009 "Wide Field Astronomy & Technology for the Square Kilometre Array", 2009

[7] Takeuchi et al 2011, General Assembly and Scientific Symposium, 2011 XXXth URSI

[8] Thornton & Border, Radiometric Tracking Techniques for Deep Space Navigation, John Wiley & Sons, Hoboken, NJ 2003

[9] Jones D. L., Folkner W. M., Jacobson R. A. et al: Astrometry of Cassini With the Vlba to Improve the Saturn Ephemeris. AJ 149, 28 2015

EPSC Abstracts
Vol. 10, EPSC2015-290, 2015
European Planetary Science Congress 2015

Investigating the Origin and Evolution of Venus with In Situ Mass Spectrometry

M. G. Trainer, P. R. Mahaffy, W. B. Brinckerhoff, N. M. Johnson, and L.S Glaze.
NASA Goddard Space Flight Center, Greenbelt, Maryland, USA (melissa.trainer@nasa.gov/ Fax: +1-301-6146104)

Abstract

Measurement of noble gas abundances on Venus remain a high priority for planetary science [1,2]. These studies are only possible through *in situ* measurement, and can be accomplished by a modern neutral mass spectrometer (NMS) such as that developed at NASA Goddard, based on flight-proven technology. Here we show how the measurement of noble gases can be secured using demonstrated enrichment techniques.

1. Introduction

The exploration of Venus continues to be a top priority of planetary science. The Planetary Decadal Survey goals for inner-planet exploration seek to discern the origin and diversity of terrestrial planets, understand how the evolution of terrestrial planets relates to the evolution of life, and explore the processes that control climate on Earth-like planets [1]. These goals can only be realized through continued and extensive exploration of Venus, the most mysterious of the terrestrial planets, remarkably different from the Earth despite the gross similarities between these "twin planets". It is unknown if this apparent divergence was intrinsic, programmed during accretion from distinct nebular reservoirs, or a consequence of either measured or catastrophic processes during planetary evolution. Even if the atmosphere of Venus is a more "recent" development, its relationship to the resurfacing of the planet's enigmatic surface is not well understood. Resolving such uncertainties directly addresses the hypothesis of a more clement, possibly water-rich era in Venus' past as well as whether Earth could become more Venus-like in the future.

Future missions will require a focused investigation of the atmospheric composition to complete the picture sketched by the probes of the 1970s and 1980s and developed further by recent missions such as Venus Express. A key issue that remains after more than 50 years of planetary exploration is the formation and evolution of the atmosphere, particularly in the context of the other terrestrial planets [2]. Comparing noble gas mixing ratios and isotopes of Venus, Earth, Mars, Jupiter, and the sun will help determine the timing and extent of atmospheric escape on Venus, a central process in planetary evolution [3]. Precise isotope systematics of Xe, an element not yet measured at Venus, can resolve uncertainties among models of the original atmospheric composition and potentially lead to a more refined understanding of the relative importance of planetary degassing on Venus, Earth, and Mars [4]. These studies are only possible through *in situ* measurement, and can be accomplished by a modern neutral mass spectrometer (NMS) such as that developed at NASA Goddard, based on flight-proven technology.

2. Instrumental Approach

Comprehensive analysis of mixing ratios and isotopic abundances of noble gases Ne, Ar, Kr, and Xe can be accomplished by the NMS by ingesting and processing atmospheric gas during a brief residence time consistent with the Pioneer Venus and Venera Probes (~1 hr.). Noble gases are typically present at low abundances in planetary atmospheres, and thus the accurate measurement of elemental and isotopic abundances presents an analytical challenge for any *in situ* instrument. Argon and neon were determined by the Venera 11/12 MS and Pioneer Venus MS to be present at approximately 70 and 7 ppm, respectively [5]. Inconsistent measurements of Kr between these missions suggest an upper limit of ≤ 100 ppb for this species, and non-detections of Xe support a similar upper limit at the ppb-level. Yet, measurements of these noble gases are necessary to constrain atmospheric evolution models. Thus, proper execution of atmospheric enrichment is needed to enhance the signal from trace noble gases and secure the required measurements with adequate precision to advance our understanding of Venus' atmospheric history.

2.1 Noble Gas Enrichment

The measurement of noble gas abundances during probe descent has been demonstrated previously by the Galileo Probe Mass Spectrometer mission into Jupiter [6,7]. GPMS used two enrichment cells to scrub the ingested atmosphere of H_2 and other active gases in order to enhance noble gases and their isotopes. These ground-breaking measurements were acquired with < 10 minutes of MS time, following ~10 minutes of gas processing during which direct MS measurements of the atmosphere were made.

For a future Venus mission, improvements to the enrichment process, pumping throughput, and instrument sensitivity over GPMS and Pioneer Venus MS would result in successful measurement of noble gas targets. Such advancements have been implemented on the Mars Science Laboratory Sample Analysis at Mars (SAM) investigation [8]. SAM's wide dynamic range quadrupole MS, and the incorporation of both scrubbers and getters into the gas manifold, effectively remove chemically active gases such as CO_2, trace noble gases from sub-picomole to nanomole abundances to be measured.

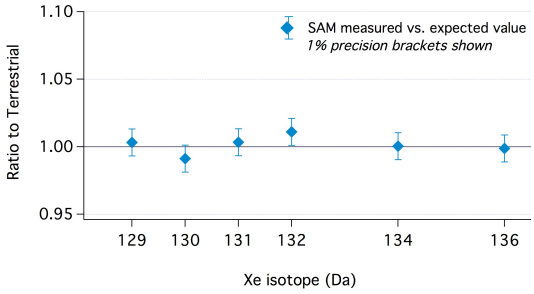

Figure 1: Static mode performance of the SAM QMS demonstrates the 1-2% precision in isotopic measurements achieved in short integration times. The entire set of measurements that generated the ratio plot in the bottom frame was acquired in 30s [8].

In particular, following enrichment of noble gases relative to the atmosphere, static mass spectrometry is utilized to maximize the signal from these low abundance, inert species. During static mass spectrometry, the quadrupole is isolated from the wide range pump, and only reactive species are pumped using a chemical getter. The resulting enrichment in heavy noble gas atoms within the analyzer enables the detection and quantitative determination of isotopic ratios with excellent precision in a short amount of time (Fig. 1).

4. Summary and Conclusions

Measurement of noble gas abundances on Venus remain a high priority for planetary science [1,2]. This can be accomplished as part of an atmospheric investigation using flight-proven technology and demonstrated enrichment techniques.

References

[1] NRC: Visions and Voyages for Planetary Science in the Decade 2013-2022, National Academies Press, Washington, DC., 2011.

[2] VEXAG: Goals, Objectives, and Investigations for Venus Exploration, 2014.

[3] Baines K. H., Atreya S. K., Bullock M. A., Grinspoon D. H., Mahaffy P., Russell C. T., Schubert G., and Zahnle K.: The atmospheres of the terrestrial planets: Clues to the origins and early evolution of Venus, Earth, and Mars. In Comparative Climatology of Terrestrial Planets (S. J. Mackwell et al., eds.), pp. 137–160, 2013.

[4] Pepin, R. O.: Atmospheres on the terrestrial planets: Clues to origin and evolution. Earth and Planetary Science Letters, Vol. 252, pp. 1-14, 2006.

[5] von Zahn, U., Kumar, S., Niemann, H., and R. Prinn:: Composition of the Venus Atmosphere, in Venus (Hunten et al eds.), pp. 299-430, 1983.

[6] Niemann, H. B., Harpold, D. N., Atreya, S. K., Carignan, G. R., Hunten, D. M., and Owen, T. C. (1992). GALILEO PROBE MASS-SPECTROMETER EXPERIMENT, Space Science Reviews, Vol. 60, pp. 111-142, 1992.

[7] Mahaffy, P. R., Niemann, H. B., Alpert, A., Atreya, S. K., Demick, J., Donahue, T. M., Harpold, D. N., and Owen, T. C.: Noble gas abundance and isotope ratios in the atmosphere of Jupiter from the Galileo Probe Mass Spectrometer, JGR-Planets, Vol. 105, pp. 15061-15071, 2000.

[8] Mahaffy P. R. et al.: The Sample Analysis at Mars Investigation and Instrument Suite, Space Science Reviews, Vol. 170, pp. 401-478, 2012.

EPSC Abstracts
Vol. 10, EPSC2015-319, 2015
European Planetary Science Congress 2015

Mapping Imaging Spectrometer for Europa (MISE)

D. L. Blaney[1], R. Clark[2], J. B. Dalton[1], A. G. Davies[1], R. Green[1], M. Hedman[3]. K. Hibbits[4], Y. Langevin[5], J. Lunine[6], T. McCord[7], C. Paranicas[4], S. Murchie[4], F. Seelos[4], J. Soderblom[8], M. Cable[1], P. Moroulis[1], Wousik Kim[1], L. Dorsky, K. Strohbehn[4], [1]NASA Jet Propulsion Laboratory, California Institute of Technology, Pasadena CA, Diana.L.Blaney@jpl.nasa.gov [2]Planetary Science Institute, Tucson AZ, [3]University of Idaho, Moscow ID, [4]Applied Physics Laboratory, John Hopkins University, Laurel, MD, [5]Institud d' Astrophysique Spatiale, Orsay, France, [6]Cornell University, Ithaca, NY, [7]Bear Fight Institute, Winthrop, WA, [8]Massachusetts Institute of Technology, Cambridge MA.

Abstract

The Mapping Imaging Spectrometer for Europa (MISE) instrument is designed to be able to unravel the composition of Europa, and to provide new insight into the processes that have in the past and continue to shape Europa, and on the habitability of Europa's ocean. The MISE design is the result of collaboration between NASA's Jet Propulsion Laboratory (California Institute of Technology) and the Applied Physics Laboratory (John Hopkins' University). JPL's Discovery Moon Mineralogy Mapper (M3) on Chandrayan-1 and APL's Compact Reconnaissance Imaging Spectrometer for Mars (CRISM) comprise the technical basis for MISE. Internal JPL and APL investments in conjunction with NASA support under the ICEE program has allowed for instrument technology development and testing to achieve a design which would perform in Europa's radiation environment and meet potential sterilization requirements due to planetary protection.

1. Science Goals

The MISE instrument is designed to enable the identification and mapping of organics, salts, acid hydrates, water ice phases, altered silicates, and radiolytic compounds at global (≤ 10 km), regional (≤ 300 m), and local scales (~ 25 m) (Figure 1). Mapping the composition of specific landforms is critical to understanding surface and subsurface geologic processes, including recent or current activity. High spatial resolution compositional mapping is also essential for detecting small outcrops of organics and salts. Distribution maps of astrobiologically relevant compounds and their geologic context can be used to assess whether Europa's ocean is capable of supporting life. MISE could provide fundamental information on where future Europa landers would have the highest probability of detecting evidence of life.

2. Instrument Description

The MISE design is for a high-optical throughput pushbroom imaging spectrometer that could observe effectively throughout a flyby or in orbit around Europa. It is designed to operate within Europa's challenging radiation environment and deal with both radiation noise and total integrated dose. MISE would cover a spectral range from 0.8–5 μm at 10 nm/channel, with an instantaneous field of view (IFOV) of 250 μrad/pixel and a swath width of 300 active pixels (Figure 2). The 0.8–2.5 μm region is essential for quantifying hydrates and bulk surface composition, while the 3–5 μm region is required for

Figure 1: Example compositional maps from imaging spectroscopy that can be used to determine the distribution of key compounds.

detecting low abundances of organics, most radiolytic products, and discriminating salts from acid hydrates. These longer wavelengths can also be used to measure thermal emissions from currently active regions.

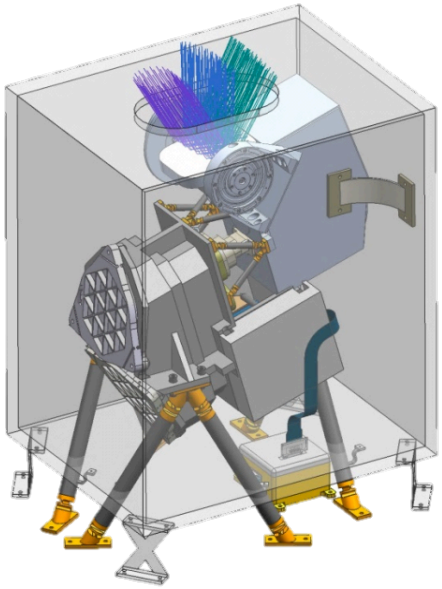

Figure 2: Model of the MISE Instrument Design.

3. Radiation and Planetary Protection Impacts on Design.

Instrument performance was required to meet potentially stringent planetary protection requirements and to operate in the Europa radiation environment. To achieve this confidence that the instrument design would work at Europa in the expected radiation environment, a prototype spectrometer was built and tested in multiple bean lines (Figure 3 and 4). The prototype included slit, grating, order sorting filter, and focal plane array utilizing the same materials and processes that MISE design incorporated. The test data was used to calibrate radiation models of expected radiation noise for the design so that appropriate levels of shielding could be utilized. The prototype also underwent a planetary protection bakeout to ensure that the design was compatible with dry heat microbial reduction (Figure 5).

Acknowledgements

The MISE instrument designed has benefitted from the work of a large number of JPL and APL engineers. Many thanks to the following for their contributions toward the design: Aboobaker Asad, Carl Bruce, Ernisto Diaz, Len Dorsky, Michael Mercury, Timothy Neville, Jose Rodriguez, Andy Santo, Elizabeth Smith, Byron Van Gorp, and Daniel Wilson.

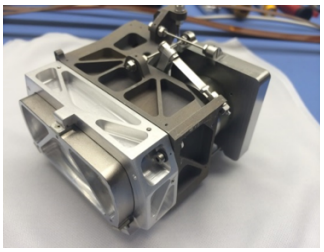

Figure 3: Prototype Spectrometer.

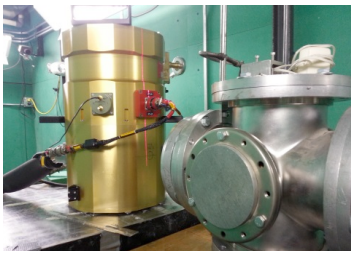

Figure 4: Prototype in radiation beamlines.

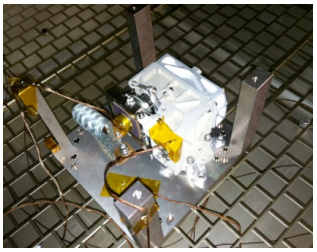

Figure 5: Prototype undergoing planetary protection bakeout.

EPSC Abstracts
Vol. 10, EPSC2015-376, 2015
European Planetary Science Congress 2015

Detectability of trace gases in the Martian atmosphere using gas correlation filter radiometry

J. A. Sinclair (1,2), P. G. J. Irwin (2), E. Wilson (3), S. B. Calcutt (2)
(1) Jet Propulsion Laboratory, California, United States (james.sinclair@jpl.nasa.gov), (2) University of Oxford, United Kingdom, (3) Goddard Space Flight Center, Maryland, United States

Abstract

We present the results of radiative transfer simulations of a gas correlation filter radiometer (GCFR) in the detection of trace species in the Martian atmosphere. We investigated two scenarios: 1) nadir and/or limb sounding from a Mars orbiter in the thermal infrared, 2) solar occultation measurements in the near-infrared from the Martian surface. In both scenarios, a GCFR would allow detection of trace gases at a lower concentration than that detectable by a conventional filter radiometer. In nadir/limb sounding, we find that CH_4, SO_2, N_2O, C_2H_2 and CH_3OH are detectable at concentrations lower than previously-derived upper limits. From solar occultation measurements, we find that CH_4, SO_2, C_2H_2, C_2H_6 are detectable at concentrations lower than previously-derived upper limits but only in low dust conditions.

1. Introduction

The atmosphere of Mars may contain a number of trace gases, which remain undetected due to their low concentrations. Outgassing from the surface, evaporation of ices, subsurface microbial metabolism and photochemical reactions in the Martian atmosphere are thought to produce a range of organic, nitrogen- and sulphur-based compounds [1,2,3]. The recent *in-situ* detection of CH_4 by Curiosity [4] is highly topical since the molecule could have a biogenic origin. However, other origins of CH_4 such as volcanism, exogenous introduction by meteorites/comets cannot be ruled out.

Some clues of the source of CH_4 could be deduced by searching for other trace gases. For example, a detection of N_2O, in addition to CH_4, may suggest a biogenic origin of CH_4 since bacteria in anoxic environments also produce N_2O [5]. Simiilarly, a detection of SO_2 and CH_4 would indicate a volcanic origin of CH_4. Other organic compounds such as C_2H_2, C_2H_6, CH_2O and CH_3OH are produced by photochemistry or oxidation of CH_4 and thus would serve as a secondary detection of CH_4. However, their lifetimes in the Martian atmosphere are much shorter than that of CH_4 and thus their presence could indicate how recent the source of CH_4.

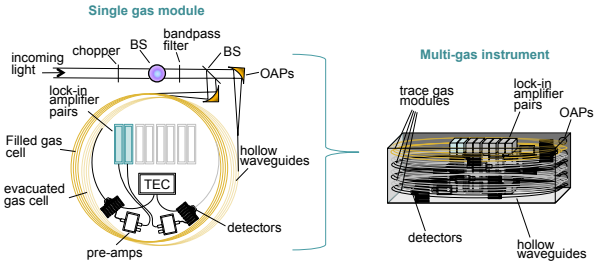

Figure 1: A top-down (left) and side-on (right) schematic of a gas correlation filter radiometer that has proven successful in laboratory tests (e.g. [6]).

Thus, there is significant scope for an instrument with the capabilities of detecting these trace gases. In this paper, we present the results of radiative transfer simulations in order to demonstrate the potential effectiveness of a gas correlation filter radiometer on a future mission to Mars.

2. Gas correlation filter radiometer

Figure 1 shows a schematic of the proposed gas correlation filter radiometer. Light from the planet (R_{source}) is viewed through a narrow band filter and then divided into two optical paths - the first containing an evacuated gas cell and the second containing a gas cell filled with the candidate gas (with a channel transmission of T_c). The average signal between the two optical paths (or wideband signal, R_w, Eq. 1) provides a measure of the overall signal from the planet atmosphere. The difference in signal between the two optical paths (or sideband signal, R_s, Eq. 2) measures the radiance only in the continuum since the filled gas cell blocks light from the planet within the absorption lines of the gas.

$$R_w = \frac{(1+T_c)}{2} R_{\text{source}} \quad (1)$$

$$R_s = (1 - T_c)R_{\text{source}} \quad (2)$$

Together, the wideband and sideband radiances allow a discrimination such that the magnitude of signal being absorbed by the gas of interest, and thus its concentration, can be determined.

3. Analysis

Radiative transfer simulatons were performed using Nemesis [7], a forward model and retrieval tool. Table 1 shows the channels in the 200 - 2000 cm^{-1} range selected for detection of each gas.

Channel	$\tilde{\nu}_0$	$\Delta\tilde{\nu}$	NESR
HDO	220	40	0.75
H_2O	240	40	0 .75
C_2H_2	730	40	0.75
C_2H_6	825	40	0.75
CH_3OH	1030	40	0.75
N_2O	1280	40	0.75
CH_4	1300	40	0.75
SO_2	1360	40	0.75
H_2CO	1740	40	0.75

Table 1: The channel centers and bandpass widths (cm^{-1}) selected for each gas and the noise-equivalent spectral radiance (NESR, in units of nW cm^{-2} sr^{-1} cm).

In a nadir viewing geometry, the concentration of each trace gas in the Martian atmosphere was increased from zero to a value such that the signal in the appropriate channel decreased by the NESR. This value in concentration was therefore deemed to be the noise-equivalent volume mixing ratio (NEVMR). Figure 2 shows the results of the NEVMRs for each gas as a function of latitude in low and high dust conditions for a gas correlation filter radiometer (GCFR) and a conventional filter radiometer (FR) for comparison. For both instruments, the lowest detectable concentration is in the northern summer hemisphere where the thermal infrared signal-to-noise ratio is highest. As shown, a GCFR allows 1) detection of all gases at lower concentrations that a FR and 2) detection of HDO, N_2O, CH_4, C_2H_2 and CH_3OH at lower than previous measured values or upper limits [8,9,10,11].

4. Summary

A gas correlation filter radiometer allows detection of trace chemical species at a lower concentration than a conventional filter radiometer. We will present similar results for an instrument performing solar occultation measurements in the near-infrared (2- to 5-μm). In addition, for both scenarios, we will also present the results of a retrieval analysis where the temperature profile, dust concentration and gas abundances are retrieved from synthetic FR and GCFR measurements.

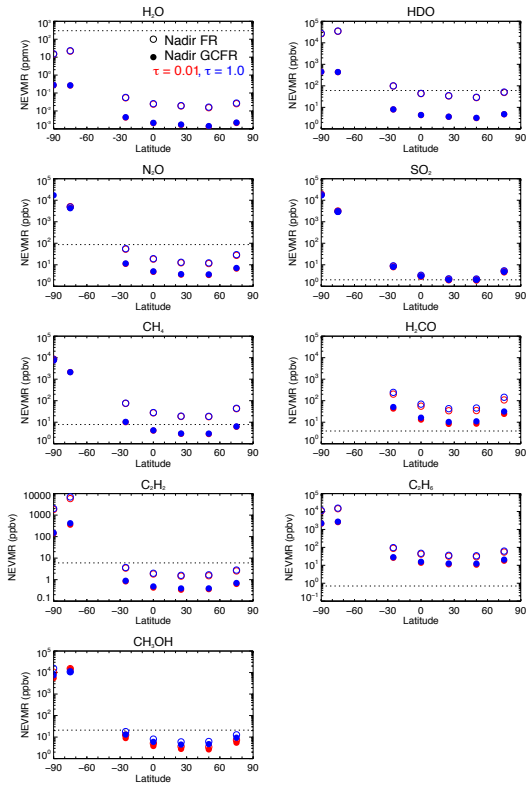

Figure 2: The noise-equivalent volume mixing ratios of each trace gas as a function of latitude in low and high dust condition (optical depths given at 3-μm). Unfilled and filled points respectively indicate the results for a filter radiometer and gas correlation filter radiometer operating in the nadir. Horizonal dashed lines indicate previously measured-abundances or upper limits.

References

[1] Atreya et al., 2007, *P&SS* 55:358-369, [2] Wong et al., 2003, *JGR (Planets)* 108:2056, [3] Wong et al., 2004, *Advances in Space Research* 33:2236-2239, [4] Webster et al., 2015, *Science* 347(6220):415-417, [5] Goreau et al., 1980, *Applied & Environmental Microbiology* 40(3):526:532, [6] Wilson et al., 2012, *Measurement Science & Technology* 22(8):085902, [7] Irwin et al., 2008, *JQSRT* 109:1136-1150, [8] Owen et al., 1982, *Advances in Space Research* 2:75-80, [9] Villanueva et al.,2013, *Icarus* 223:11-27, [10] Webster et al., 2013, *Science* 341:260-263, [11] Encrenaz et al., 2011, *A&A* 530:A37.

EPSC Abstracts
Vol. 10, EPSC2015-378, 2015
European Planetary Science Congress 2015

Near-Subsurface Science from a Digital Beamforming Polarimetric Synthetic Aperture Radar

L. M. Carter and R. F. Rincon
NASA Goddard Space Flight Center (lynn.m.carter@nasa.gov)

Abstract

Many important questions in planetary science depends on our ability to detect and map surface and subsurface layers of planetary bodies. We are developing a P-band (435 MHz, 70 cm wavelength) digital beamforming radar, called Space Exploration SAR (SESAR), capable of providing the measurement flexibility needed to address multiple types of science goals. SESAR will provide high spatial resolution imaging, full polarimetry, multi-beam scatterometry and altimetry of planetary targets such as the Moon and Mars by using beamforming technology that can adjust the radar experiment to meet the specific science goals of each target.

1. Introduction

Planetary science objectives include mapping the surfaces and near-surfaces of planets to determine how they are shaped through different processes (volcanism, cratering, fluvial activity, etc.), comparing the development and evolution of cryospheres across planets, determining how regoliths develop through time, and locating regions that are (or were) hospitable to life. Low frequency Synthetic Aperture Radar (SAR) is the only remote sensing technique capable of imaging buried surfaces at meter-scale spatial resolution.

The SESAR instrument will be modular and can be easily adapted for Discovery (or New Frontiers) missions to the Moon, Mars, Mercury, Venus, and asteroids (including Ceres and Phobos).

The lunar surface is covered in a ~2-10 m of regolith (dust and small rock mixture). SESAR will be able to image through the regolith to characterize the near-surface stratigraphy of the Moon in unprecedented detail not available to any other instrument. P-band radar data acquired with Earth-based systems have revealed rough buried flows in mare regions that are not visible to any other type of instrument [1]. SESAR will also be able to image buried channels [1] and possibly detect near-surface lava tubes.

Locating habitable regions, finding water, and determining the evolution of the Martian cryosphere are primary goals of Mars exploration. Because water and all ice outside of the polar regions is buried, radar is a key technology for cryosphere studies. Radar also has a long history of detecting buried fluvial channels on the Earth and Mars and could be used to search for these features in the upper tens of meters of the Martian surface.

2. Radar Parameters

Using a P-band wavelength will ensure that SESAR will image features below 2-3 m (and as much as 10-15 m) of surface cover on the Moon and Mars (Fig. 1), and many tens of meters into water ice on Mars. P-band is an ideal wavelength because it provides high-resolution, meter-scale imaging, and it will not

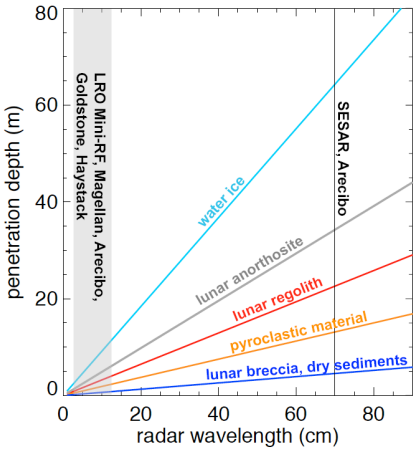

Figure 1 SESAR will have a greater penetration depth than most prior radars (orbital and Earth-based). Penetration depth is defined as the point at which the wave power has been reduced by 1/e relative to original power.

reflect from centimeter-sized rocks that are prevalent in near-surface regolith.

SESAR's polarimetric data products will provide important information about the nature of the surface and subsurface that cannot be obtained solely with backscatter power images [2]. SESAR's polarimetry will also be critical for distinguishing mantling deposits from smooth uncovered surfaces, and for determining the roughness and continuity of geologic units.

3. Instrument Concept

The SESAR instrument employs a modular approach that allows for the customization of the instrument architecture to meet scientific mission requirements for a specific planetary body. The modular approach distributes the radar key systems into instrument panels composed of active subarrays, as illustrated in Fig 2.

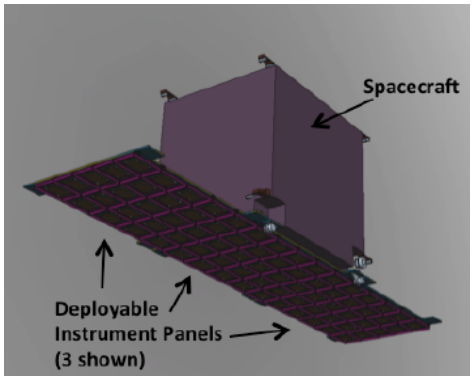

Figure 2 SESAR's distributed architecture enables instrument customization for a given planetary mission, and the implementation of advanced operational modes.

SESAR's architecture will be fully programmable and capable of multi-mode radar operation including unprecedented polarimetric SAR imaging, nadir SAR altimetry, and scatterometry. Some of its advanced programmable features include single, dual, or full polarimetry; multi-look angle data collection: simultaneous left and right of the track imaging; selectable resolution and swath width; digital beam steering (no moving parts); and beam pattern control; among others.

One of SESAR's main features will be its operation using electronic beamforming on transmit, and digital beamforming on receive [3]. Both beamforming techniques employ interference among the signals from each of the radar antenna subarrays to generate far-field beam patterns with predefined and selectable look angles, beamwidths and sidelobe levels, and without the use of moving parts.

Using beamforming, SESAR will be able to synthesize multiple antenna beams, simultaneously or interleaved, permitting the implementation of non-conventional imaging that can overcome fundamental limitations of conventional radar systems [3,4]. Some of its benefits include an increase in the measurement swath without reducing the received antenna gain, and the suppression of ambiguities or localized interference in the receiver signal by appropriate null-steering of the antenna pattern. The antenna gain, beam pointing angle, and sidelobe structure can be programmed in real-time for specific tasks. Furthermore, multiple beams can be synthesized on both sides of the flight-track, as well as nadir, using a single nadir-looking antenna, thus increasing the coverage area.

In the SAR imaging mode, SESAR will image the ground with fine resolution pixels in the order of up to 2 m over one or multiple beams to permit geologic analysis. Each of the beams will measure up to four polarizations to facilitate retrieval of the Stokes parameters, from which a broad suite of scattering mechanisms associated with particular geological processes can be assessed.

6. Summary and Conclusions

The digital beamforming and full polarimetry capabilities of SESAR will provide a very flexible radar system that can be used to tailor radar experiments to the science questions for a given planetary target.

References

[1] Campbell, B. A. et al., J. Geophys, Res., 119, 313, doi:10.1002/ 2013JE004486, 2014.

[2] Carter, L. M. et al., Proc. IEEE, doi:10.1109/ JPROC.2010.2099090, 2011.

[3] Rincon, R. F. et al., IEEE Transactions on Geosci and Rem. Sens., vol.49, no.10, pp.3622-3628, Oct. 2011 doi: 10.1109/TGRS.2011.2157971, 2011.

[4] Krieger, G. et al., Trans. Geosci. Remote Sensing, vol. 46, No. 1, pp. 31 – 46, 2008.

EPSC Abstracts
Vol. 10, EPSC2015-388, 2015
European Planetary Science Congress 2015

Net Flux Radiometer for a Saturn Probe

S. Aslam (1), M. Amato (1), D. H. Atkinson (2), A. Colaprete (3), T. Hewagama (1), D. E. Jennings (1), J. I. Lunine (4), C. A. Nixon (1), A. A. Simon-Miller (1), O. Mousis (5), G. T. Quilligan (1) and E. J. Wollack (1)
(1) NASA Goddard Space Flight Center, Greenbelt, MD 20771, USA (shahid.aslam-1@nasa.gov / Fax: +1-301-2861683); (2) Department of Electrical and Computer Engineering, University of Idaho, Moscow, Idaho, USA; (3) NASA Ames Research Center, Moffet Field, CA 94035, USA; (4) Center for Radiophysics and Space Research, Space Sciences Building Cornell University, Ithaca, NY 14853, USA; (5) Aix Marseille Universit´e, CNRS, Laboratoire d'Astrophysique de Marseille, UMR 7326, 13388, Marseille, France

Abstract

A Net Flux Radiometer (NFR) concept is presented that can be included in an atmospheric structure instrument suite for any future NASA or ESA led Saturn Probe Mission. The current design has two spectral channels i.e., a solar channel (0.4-to-5 µm) and a thermal channel (4-to-50 µm). The NFR is capable of viewing five distinct viewing angles during the descent. Non-imaging Winston cones with window and filter combinations define the spectral channels with a 5° Field-Of View (FOV). Uncooled thermopile detectors are used in each spectral channel and are read out using a custom designed Application Specific Integrated Circuit (ASIC).

1. Introduction

Two notable instruments have flown in the past namely, the Large Probe Infrared Radiometer (LIR) [1] on the Venus Probe, and the Net Flux Radiometer (NFR) on the Galileo Probe [2]. The NFR builds on the lessons learned from the Galileo Probe NFR experiment and is designed to measure the net radiation flux within Saturn's harsh atmosphere [3]. The nominal measurement regime for the NFR extends from ~0.1 bar (near the tropopause) to at least 10 bars, corresponding to an altitude range of ~79 km above the 1 bar level to ~154 km below and a temperature excursion of ~85 K to ~300 K. The NFR measures the radiative energy anisotropies with altitude. In the solar channel the downward flux will determine the solar energy deposition profile and the upward flux will yield information about cloud particle absorption and scattering. In the thermal channel the net flux will define sources and sinks of planetary radiation. In conjunction with calculated gas and particulate opacities, these observations will determine the atmosphere's radiative balance.

2. Radiometer Concept

The NFR, Fig. 1, measures upward and downward radiation flux in a 5° FOV at five distinct viewing angles; ±80°, ±45°, and 0°, relative to zenith/nadir.

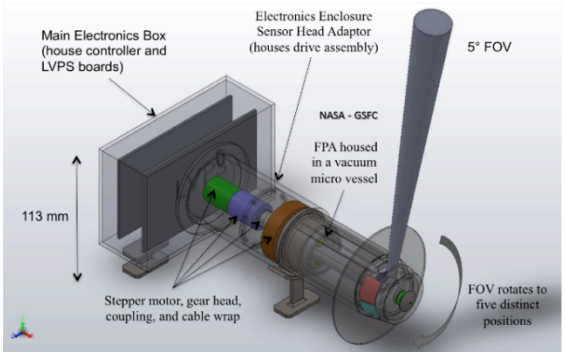

Figure 1: NFR instrument concept showing a 5° FOV that can be rotated by a stepper motor into five distinct look angles.

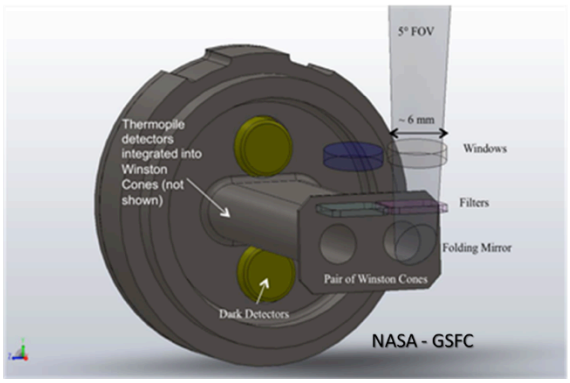

Figure 2: NFR focal plane assembly showing the dual Winston cone assembly to limit the exacting FOV in each channel. The windows and filters define the solar and thermal spectral channels.

The Focal Plane Assembly (FPA), Fig. 2, is comprised of bandpass filters, folding mirrors, non-imaging Winston cone concentrators, and radiation hard uncooled thermopile detectors housed in a windowed vacuum micro-vessel that is rotated to the viewing angle by a stepper motor. Assuming a thermopile voltage responsivity of 295 V/W, an optical efficiency of 50%, a detector noise of 18 nV/√Hz and an ASIC input referred noise of 50 nV/√Hz with 12-bit digitization gives a system signal-to-noise ratio of 300 to 470 in the solar spectral channel and 100 to 12800 in the thermal spectral channel for atmospheric temperature and pressure ranges encountered in the descent, i.e., ~85 to 300 K and 0.1 to 10 bar respectively.

2. Radiometer Readout

A physical and functional block diagram of the NFR is shown in Fig. 3. The focal plane consists of four single pixel thermopile detectors (solar, thermal and two dark channels), bandpass filters and Winston concentrators. The Front End Electronics (FEE) readout, Fig. 4, uses a custom radiation-hardened-by-design mixed-signal ASIC for operation with immunity to 174 MeV-cm^2/mg single event latch-up and 50 Mrad (Si) total ionizing dose. The ASIC has sixteen low-noise chopper stabilized amplifier channels that have configurable gain/filtering and two temperature sensor channels that multiplex into an on-chip 16-bit sigma-delta analog-digital converter (SDADC). The ASIC uses a single input clock (~1.0 MHz) to generate all on-chip control signals such as the chopper/decimation clocks and integrator time constants. The ASIC also contains a radiation tolerant 16-bit 20 MHz Nyquist ADC for general-purpose instrumentation needs.

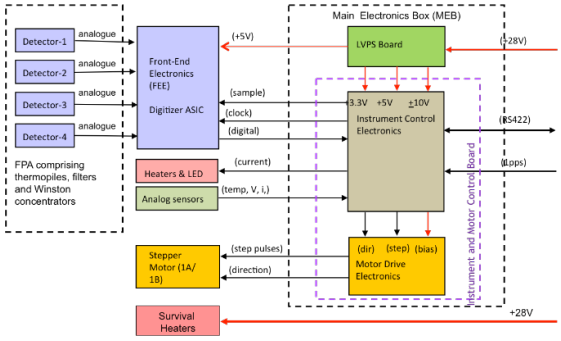

Figure 3: NFR block diagram showing the major subsystems and Probe interfaces.

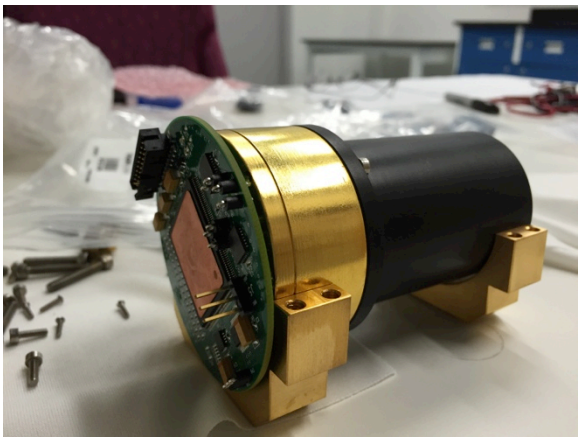

Figure 4: NASA GSFC is testing early engineering models of the critical components the NFR. Dual Winston cone assembly and thermopile FEE readout (diameter ~ 70mm) that uses a GSFC rad-hard mixed-signal ASIC.

3. Volume, Mass, Power, Data Rate

Mass: ~2.4 kg
Volume: ~113 mm x 144 mm x 279 mm
Basic Power: ~5 W
Average Data Rate: ~55 bps
Total Data Volume: ~297 kbits (90-minutes)

4. Summary and Conclusions

NASA GSFC has designed a NFR that will be suitable for integration into an atmospheric instrument suite on-board a future Saturn Probe Mission. Relaxing the FOV to 7° will enable the use of thermopile detectors with smaller integrated optics allowing the NFR focal plane design to incorporate up to seven channels with an overall reduction of volume and mass.

References

[1] Boese, R. W., et al. 1980. The Infrared Radiometer on the Sounder Probe of the Pioneer Venus Mission, IEEE transactions on Geoscience and Remote Sensing, vol. GE-18, no. 1.

[2] Sromovsky, L.A. 1998. Galileo probe measurements of thermal and solar radiation fluxes in the Jovian atmosphere, Journal of Geophysical Research, vol. 103, no. E10, pp. 22929-22977.

[3] Mousis, O., et al. 2014. Scientific Rationale and concepts for an In Situ Saturn Probe, EPSC Abstracts, Vol. 9, EPSC2014-437-1 (and references therein).

EPSC Abstracts
Vol. 10, EPSC2015-416, 2015
European Planetary Science Congress 2015

Demonstration of Longevity of Microdevices for *in situ* Analysis of Organic Molecules on Outer Planet Icy Moons

Z. A. Duca (1), G. K. Tan (1), T. P. Cantrell (1), M. A. Van Enige (1), R. A. Mathies (2), and A. M. Stockton* (1)
(1) Georgia Institute of Technology, GA, USA, (2) University of California, Berkeley, CA, USA (astockto@gatech.edu)

Abstract

Quantitative compositional *in situ* analysis of small organic molecules in extraterrestrial environments provides essential information on planetary formation and evolution, as well as the capability to find potential signatures of past or present life. Microchip capillary electrophoresis (µCE) with laser-induced fluorescence (LIF) detection has proven to be capable of highly sensitive (sub parts-per-trillion, or pptr) automated quantitative compositional analysis of multiple organic compound classes. Here, we demonstrate the retained functionality of automated µCE-LIF microdevices fabricated in 2005. After 5 hours of vacuum cycling, a pneumatically-controlled valve re-opened and regained normal use. The ability of these microdevices to retain functionality after over 10 years of storage combined with system sensitivity, reliable autonomous control, and chiral resolution further supports the value of µCE-LIF as an *in situ* technique for outer planetary missions.

1. Background: µCE-LIF for Planetary Exploration Missions

The ability to obtain quantitative compositional analysis of small organic extraterrestrial molecules *in situ* can enable the acquisition of essential information on planetary formation and evolution, as well as the capability to find potential signatures of past or present life. However, due to lengthy mission transit times, the requirement for automated control, and the costs and risks associated with space flight, the development of new organic analytical technologies for outer planetary missions have been limited. MicroCE-LIF is an emerging technology under development that enables highly sensitive (sub pptr), automated, and quantitative compositional analysis of multiple organic compound classes, [1] including amines,[2] amino acids,[3] aldehydes,[4] ketones, carboxylic acids, [5] thiols, [6] and polycyclic aromatic hydrocarbons.[7]

While µCE-LIF systems have been proposed for missions to Mars (Mars Organic Analyzer, or MOA), Enceladus (Enceladus Organic Analyzer), and Europa (Ice Shell Impact Penetrator), little has been done to raise the technology readiness level (TRL) of the microdevice itself.

Resources for outer planetary space flight are limited. The high costs of sample return and extreme risks associated with a lengthy mission flight times force the use of autonomously-controlled, *in situ* techniques. With the additional requirement for highly sensitive quantitative compositional analysis to truly gain insight from organic composition, few techniques are capable of meeting these needs. As demonstrated extensively in the laboratory[8] and the field,[9] µCE-LIF meets these needs in a unique and powerful way. However, in order to fully demonstrate the capability of the µCE system to complete an entire mission successfully and raise the TRL to the point where the instrument could be readily put on a mission payload, the microvalves must be demonstrated to function efficiently after a 9-10 year space flight, in addition to being able to withstand extreme temperature, pressure, and vibrational conditions.

2. µCE-LIF Microdevice Longevity

Automation of µCE-LIF systems is achieved using pneumatically-actuated microfabricated monolithic membrane microvalves (Figure 1). Microvalves consist of a discontinuous fluidic channel etched in a glass substrate with a displacement chamber etched in a pneumatic layer opposite the fluidic layer across

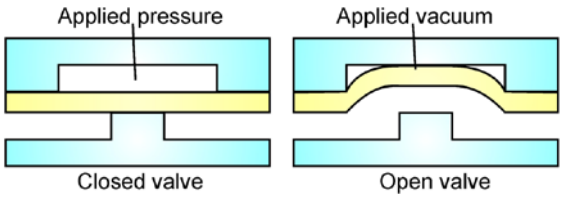

Figure 1: Cross-section of a pneumatically-actuated monolithic membrane microvalve.

Figure 2: Rigid mount holding a 10+ year old automated µCE-LIF microdevice.

an elastomeric membrane. When a vacuum is applied to the displacement chamber, the membrane deflects, drawing fluid into the resulting chamber and enabling fluidic flow across the discontinuity. Upon the application of a mild pressure to the displacement chamber, the membrane deflects again, forcing fluid out of the valve through the nearest open fluidic connection. Multiple valves in series operated sequentially form a peristaltic pump, and digital arrays of these microvalves enable complex microfluidic processing with operations including metering, mixing, dilution, reaction, etc…

To investigate the effect of an outer planetary mission flight time on automated µCE-LIF microdevices, microdevices fabricated in the UC Berkeley Microfabrication Laboratory were stored unused for 10+ years. After this time, the microdevices were housed in a custom-built rigid mount for testing (Figure 2). The mount enabled air-tight connection between the microdevice and the off-chip pneumatic control system and steadied the microdevice to enable constant video capture during valve cycling. Valves were opened by cycling the following process: apply a -0.750 bar pulse for 500 miliseconds (ms), let return to standard pressure for 500 ms. Actuation was controlled via a custom program installed on an Arduino, which in-turn regulated a custom-built electronic circuit, which then controlled a custom-built pneumatic circuit that used a Lee Company solenoid valve to switch between vacuum and ambient pressure.

Figure 3 shows the opening of a valve over 5 hours of repeated cycles. When open, the shadow of the valve appears more bubble-like, giving off a stronger reflection. When tested on a colored fluidic sample, no bleed of fluid into the pneumatic control line was observed, even after continuous and prolonged operation, indicating that the elastomeric membrane

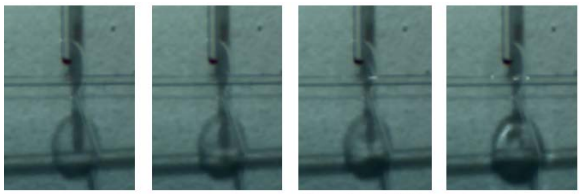

Figure 3: Photographs of valve opening.

remained intact during both prolonged storage and throughout the opening protocol. The opening of these valves after repeated cycling shows retained functionality even after over 10 years of storage time, which is a significant result towards increasing the TRL of µCE-LIF microdevices.

3. Summary and Conclusions

The µCE-LIF system for detecting and analyzing organic compounds could prove to be an essential tool in the search for life elsewhere in the solar system. Previous work has shown that automated µCE-LIF gives sub-pptr sensitivity and chiral analysis of organic compounds. The work reported here showing that microdevice functionality is retained after 10+ years of storage is a significant step towards acceptance of this technology for space flight. Further work will demonstrate microdevice functionality after extreme swings in temperature, pressure, and vibrational conditions.

Acknowledgements

Alison Skelley, Will Grover and Robin Ivester could not have anticipated when they designed and fabricated the devices that they would be used in this work over a decade later.

References

[1] Kim, J., *et al.*, *Anal. Chem.*, 85, 7682-7688, 2013.
[2] Cable, M., *et al.*, *Anal. Chem.*, 85, 1124-1131, 2013.
[3] Chiesl, T., *et al.*, *Anal. Chem.*, 81, 2537-2544, 2009.
[4] Stockton, A., *et al.*, *Electrophoresis*, 31, 3642-3649, 2010.
[5] Stockton, A., *et al.*, *Astrobiology*, 11, 519-528, 2011.
[6] Mora, M., *et al.*, *Electrophoresis*, 34, 309-216, 2013.
[7] Stockton, A., *et al*., *Anal. Chem.*, 81, 790-7906, 2009.
[8] Skelley, A., *et al*., *PNAS U.S.A.*, 102, 1041-1046, 2005; Benhabib, M., *et al.*, *Anal. Chem.*, 82, 2372-2379, 2010.
[9] Skelley, A., *et al.*, *JGR*., 111, G04S11, 2007.

EPSC Abstracts
Vol. 10, EPSC2015-589, 2015
European Planetary Science Congress 2015

Radiation mitigation in the Particle Environment Package (PEP) sensors for the JUICE mission

S. Barabash (1), S. Karlsson (1), M. Wieser (1), P. Brandt (2), J. Westlake (2), P. Wurz (3), M. Fränz (4)
(1) Swedish Institute of Space Physics, Kiruna, Sweden; (2) John Hopkins University / Applied Physics Laboratory, Laurel, USA; (3) University of Bern, Bern, Switzerland; (4) MPI fuer Sonnensystemforschung, Götingen, Germany.
(stas.barabash@irf.se / Fax: +46-980-79025)

Abstract

PEP (Particle Environment Package) is a suite of 6 (six) sensors measuring ions, electrons, exospheric neutral gas, thermal plasma and energetic neutral atoms present in all domains of the Jupiter system. Mitigation of the Jovian penetrating radiation is the outstanding problem of all PEP sensors design. We present results of the radiation simulations and the main design solutions that allow us to reach signal-to-noise ratios sufficient to address the PEP science objectives and decrease the total ionization dose below 100 kRad over the whole mission.

1. PEP suite

PEP measures positive and negative ions, electrons, exospheric neutral gas, thermal plasma and energetic neutral atoms present in all domains of the Jupiter system over nine decades of energy from < 0.001 eV to > 1 MeV with full angular coverage. The six PEP sensors are:

- Jovian plasma Dynamics and Composition analyzer (JDC);
- Jovian Electrons and Ions analyzer (JEI);
- Jovian Energetic Electrons (JoEE);
- Jovian Energetic Neutrals and Ions sensors (JENI);
- Jovian Neutrals Analyzer (JNA);
- Neutral gas and Ion Mass spectrometer (NIM).

Mechanically the sensors are arranged in 4 units which are grouped in two groups PEP-Lo and PEP-Hi (Fig. 1).
As particle detectors PEP uses ceramic channel electron multipliers (CCEM) and microchannel plates (MCP). The detectors are sensitive to the penetrating radiation and measurements of the required particle fluxes to achieve the PEP scientific objectives require comprehensive radiation mitigation measures.

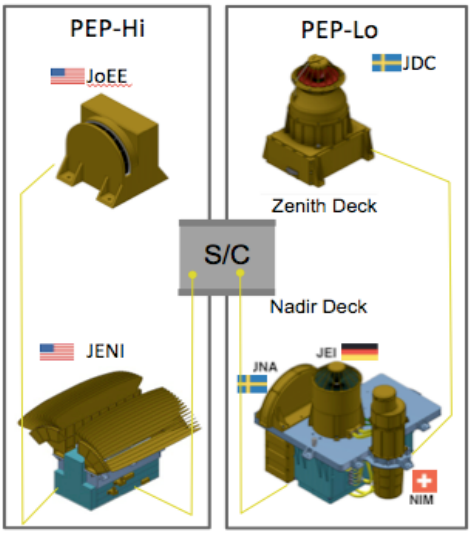

Figure 1: PEP suite and PEP sensors

2. Jupiter radiation

Jupiter possesses the strongest radiation belts in the solar system. The JUICE mission operating as close to Jupiter as Europa will experience significant fluxes of penetrating radiation, mostly electrons (Fig. 2).

The energetic electrons interacting with the instrument shielding and structure result in significant fluxes of secondary gamma rays in the energy range up to 10 MeV. The fluxes of gammas may exceed the fluxes of electrons at the detector locations by a factor of 10.

Fluxes of other particles, for example energetic protons, are significantly lower.

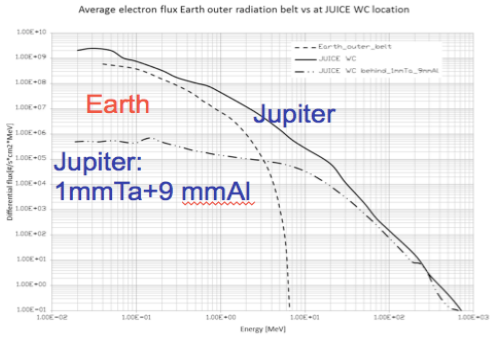

Figure 2: Comparison of energetic electrons fluxes at Europa and the Earth radiation belt.

3. PEP radiation mitigation

PEP radiation mitigation strategy includes *(1)* passive shielding to reduce total dose and backgrounds, *(2)* coincidence schemes to increase signal-to-noise ratio (SNR), *(3)* reduction of the detector sensitive area to reduce background rates keeping foreground sensitivity same by employing focusing electrostatic optics, *(4)* reduction of the sensor volumes to decrease the internal surface areas emitting not-valid secondary electrons, *(5)* monitoring instantaneous background rates to be subtracted, *(6)* where feasible, replacement of microchannel plates (MCP) by Ceramic Channel Electron Multipliers (CCEM), which are much less radiation sensitive,. MCPs are still used when imaging is required and the radiation can be mitigated by multiple coincidences.

The passive shielding includes spot shielding of individual electrical components and shielding elements shared by sensors and subsystems. Comprehensive radiation modelling was performed to optimize the shielding geometry and graded shielding design. The average doses achieved for electronics are below 100 kRad (including the Environmental Safety Factor that is equal to 2). The tools used in the analysis are: GRAS FMC (Geant4 Radiation Analysis for Space, Forward Monte Carlo), GRAS RMC (Geant4 Radiation Analysis for Space, Reversed Monte Carlo), SSAT (Sectoring Shielding Analysis Tool), FASTRAD, by TRAD, which includes ray-tracing, RMC and NOVICE interface.

The coincidence methods used in PEP sensors are based on *(1)* ToF coincidence, *(2)* anti-coincidence, *(3)* matching particle energy measured independently, *(4)* matching detector hit position measured independently (Table 1). The ToF coincidence is the most effective way to increase signal-to-noise ratio (SNR) because the probability of two non-correlated background events to occur within a short TOF window (from a few ns to 512 ns) is relatively low. Anti-coincidence schemes used in PEP rely on anticoincidence between valid events and background events recorded by anti-coincidence solid state detectors (SSD). PEP also uses the difference in pulse-height distributions (PH) from valid and penetrating particles detected by an MCP.

Table 1: PEP coincidence schemes

	JDC	JEI	JoEE	JENI	JNA	NIM
ToF coincidence	1x			2x	1x	1x
Anti-coincidence	1x	1x	1x			
Matching energy			1x			
Matching position				1x	1x	
Total coincidence	2	1	2	3	3	1
PH threshold	1x			1x	1x	

EPSC Abstracts
Vol. 10, EPSC2015-726, 2015
European Planetary Science Congress 2015

The SEIS Experiment for the Insight Mission: Development and management plan

Ph.Laudet[1], Ph. Lognonné[2] , W.B.Banerdt[3], S DeRaucourt[2], F.Ijpelaan[1], L.Kerjean[1], G.Pont[1], A.Sylvestre-Baron[1], N.Verdier[1], J.Feldman[3], K.Hurst[3], J.Kastner[3], K.Klein[3], D.Giardini[5], P.Zweifel[5], C.Bramanti[6], W.T.Pike[7], S.Calcutt[8], D.Mimoun[4], M.Bierwirth[9], U.Christensen[9] and the SEIS team

[1]CNES, Toulouse, France, (philippe.laudet@cnes.fr) , [2]Département de Géophysique Spatiale et planétaire, IPGP, Paris, France (lognonne@ipgp.fr), [3]Jet Propulsion Laboratory, Pasadena, California, USA (william.b.banerdt@jpl.nasa.gov), [4]Institut Supérieur de l'Aéronautique et de l'Espace Name, Toulouse, France, [5]ETH, Zürich, Switzerland, [6]ESA/Prodex Noordwijk, NL, [7]Imperial College, London, UK, [8]Oxford University, Oxford, UK, [9]MPS, Göttingen, Germany,

Abstract

SEIS is a Mars seismometer, provided by CNES to JPL to be the threshold instrument of the next Mars mission, InSight, to be launched by NASA in March 2016.

Discovery missions leads to a very strict frame of development, where schedule is driving development and qualification plans.

We will explain how this constraint has been taken into account during development phases, until delivery of flight model, with a context of international cooperation without exchange of founds between partners.

1. Introduction

The Insight NASA Discovery mission, led by the Jet propulsion Laboratory, will deploy in September 2016 a very broadband seismometer on the Mars surface, SEIS (Seismic Experiment for Interior Structure). It is an hybrid 3-axes instrument, which joins 3 very broadband oblique sensors with 3 short period sensors. The sensor assembly and its wind and thermal shield will by deployed on the Mars surface from a Phoenix-like lander by a robotic arm (IDS). The acquisition system will be hosted in the spacecraft warm electronics box, and connected to the deployed sensor assembly by a tether. The SEIS experiment is provided by CNES, the French Space Agency, which manages a wide consortium including IPGP of Paris, Imperial College of London, Oxford University, MPS of Göttingen, ETH of Zürich, ISAE from Toulouse and the Jet Propulsion Laboratory of Pasadena.

In addition to the seismometer, the Insight payload will also include a suite of instruments complementary to the seismometer, such as a precision temperature sensor, a micro-barometer, a magnetometer and a wind sensor, making it the first broadband seismic broadband station on another planet. A heat flow sensor and geodetic measurements will provide additional science measurements, in order to constrain the internal structure of Mars.

Several challenges have been overcome to design and realize the planetary seismometer, which will exhibit a self-noise of about 10^{-9} m/s^2/sqrt(Hz) in its seismic bandwidth for the very broadband component. These challenges implied a very complex hardware, both from a mechanical point of view and from an electronic point of view. Due to programmatic context of this NASA mission, deadlines were very short, and the development plan had to be driven by schedule. Qualification phases of the instrument and its sub-systems had to be shortened and parallelized.

Also, specific attention has been paid to the organization of the consortium that was in charge to deliver the SEIS instrument, and to the consequences of such a wide collaboration schema on the development plan.

3. Figures

Below, is a symbolic picture of the consortium, and interfaces between partners.

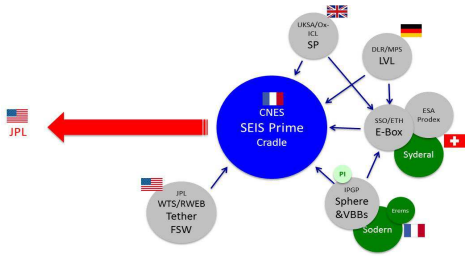

6. Development and qualification plan driven by schedule

We will present all type of concerns that have been met due to schedule driven activities, consortium organization, associated risks, and how we have mitigated them.

This can be taken as lesson learns for scientific instruments developed in a similar context.

EPSC Abstracts
Vol. 10, EPSC2015-769, 2015
European Planetary Science Congress 2015

Enceladus Icy Jet Analyzer (ENIJA) : Search for life with a high resolution TOF-MS for in situ characterization of high dust density regions

R. Srama (1,2), F. Postberg (3), H. Henkel (4), T. Klopfer (1), Y. Li (1), J. Simolka (1), S. Bugiel (1), S. Kempf (5) , J. Hillier (6), N. Khawaja (3), M. Trieloff (3), B. Abel (7), G. Moragas-Klostermeyer (1), H. Strack (1), J. Schmidt (8), R. Soja (1), Z. Sternovsky (5), T. Spohn (9)
(1) Institute of Space Systems, IRS, Univ. Stuttgart, Ger (srama@irs.uni-stuttgart.de) (2) Baylor Univ., Waco, TX, USA, (3) Univ. Heidelberg, Ger, (4) vH&S, Schwetzingen, Ger, (5) Univ. of Colorado, Boulder, USA, (6) Univ. Kent, Canterbury, UK, (7) IOM, Leipzig, Ger, (8) Univ. Oulu, F, (9) DLR Berlin, Ger

Abstract

ENIJA was developed to search for the prebiotic molecules and biogenic key compounds like amino acids in the plumes of Saturn's moon Enceladus. ENIJA records time-of-flight mass spectra in the range between 1 and 2000 u produced by high-velocity impacts of individual grains onto a metal target. The spectrometer has a measurement mode for cations or anions formed upon impact, with concurrent determination of the mass of the detected grains. Detection of elemental and molecular species over such a wide mass range permits clear characterization of particle chemistry, simultaneously covering individual ions like H^+, C^-, O^- and complex organics with masses of many hundred u. ENIJA is sensitive to water ice, minerals, metals, organic particles, and mixtures of these components. The instrument is based on the principle of impact ionization and optimized for the analysis of high dust fluxes and number densities as typically occur during Enceladus plume crossings or in cometary comae. The mass resolution is m/dm > 970 for typical plume particles in the size range 0.01 to 100 µm. The instrument mass and peak power is 3.5 kg and 14.2 W, respectively. The instrument is part of the model payload for the mission „Enceladus Life Finder“ (ELF).

1. Scientific Performance

The core of the Enceladus Icy Jet Analyzer (ENIJA) is a time-of-flight mass spectrometer for the compositional analysis of submicron and micron-sized dust particles. Most of the ice particles in Enceladus' plume have been shown to be direct samples of subsurface waters. In contrast, the plume gas probably reflects a mixture of outgassing from water and ice. To get a meaningful picture of Enceladus' geochemical and astrobiological potential both emitted phases, solid and gas, have to be analyzed.

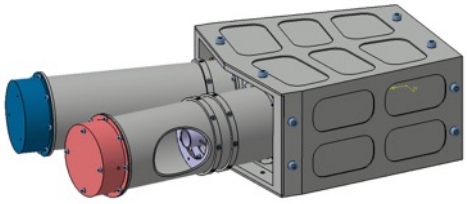

The high mass resolution enables a clear separation of isotopes for all singly charged elements. Multiply charged ions (e.g. Mg^{2+}, O^{2-}) are not expected for dust impact velocities below 20 kms^{-1}. Cluster ions with higher masses will be abundant species since they preferably form at impact velocities below 10 kms^{-1}. This was shown by the Cosmic Dust Analyzer (CDA) onboard Cassini, with which measurements of plume particles showed that salt bearing icy particle impacts generate molecular clusters like $(H_2O)_nNa^+$, $(NaOH)_nNa^+$, $(NaCl)_nNa^+$, or $(Na_2CO_3)_nNa^+$. These sequences actually revealed the quantitative composition of their liquid sources. Although CDA was by no means optimized for high fluxes of dust and gas in Enceladus' plume, it achieved outstanding results by adaptable instrument operation. In contrast, the ENIJA instrument will be optimized for Enceladus plume measurements. With 5 times lower instrument mass it provides an improved spectrum mass resolution (factor 40), maximum flux (factor 100), sensitivity (factor 100), and spatial resolution (factor 50). The high spatial resolution of ENIJA is based on its high

rate operational mode (up to 50 spectra are recorded per second) and accurate impact time information (1/256 s). An Enceladus flyby speed of about 5 km s^{-1} therefore provides a spatial accuracy of less than 20 m, allowing precise determination of compositional profiles along the spacecraft trajectory.

Impact ionization is used as the basic physical principle to characterize individual dust particles. This process is well understood and shows an unsurpassed sensitivity for compounds embedded in a water ice matrix. As has been demonstrated by CDA, salts and other minerals can be identified at ppb level. All organic compounds can be quantified at 10 ppm and below (see lab spectrum above). It could be demonstrated that some polar organic species, like many amino acids, can be quantified down to 1 ppb.

Due to its small target area (smaller capacitance) and better electrical screening, ice particles as small as 0.1 µm (at an impact speed of 5 km s^{-1}) can be analyzed. As this detection threshold scales with impact speed, faster impacts, such as from silica stream particles originating from Enceladus, can be investigated down to the nanometer scale. An optional independent ENIJA subsystem running parallel to the spectrometer during Enceladus encounters is the "High Flux detector" (HFD). It measures fluxes up to 10^8 s^{-1} m^{-2}. This instrument will map the dynamical profile (number density, ejection speeds, and size distribution) of Enceladus' ice jets.

2. Instrument Description

The main system of ENIJA is a reflectron-based impact-ionization time-of-flight mass spectrometer for the detection of individual hypervelocity dust impacts. Major improvements with respect to former dust spectrometers like PIA (Giotto), CIDA (Stardust) or CDA (Cassini) are: a lower weight, a higher mass resolution, a higher impact recording rate, an iridium target with efficient target heating, an instrument cover (CIDA had no instrument cover), and improved background noise.

The reflectron has a depth of 170 mm and the angle between the arms is 20 degrees. The instrument is composed of one reflectron with potential rings and two drift tubes. One tube contains the impact target and the second contains the ion detector. Dust particles enter the target section via an aperture. The aperture is sealed before launch and during cruise phase with a cover which protects the instrument from contamination.

A hypervelocity particle impact generates an impact plasma and the electrical potential of 2000 V between target and acceleration grid separates the

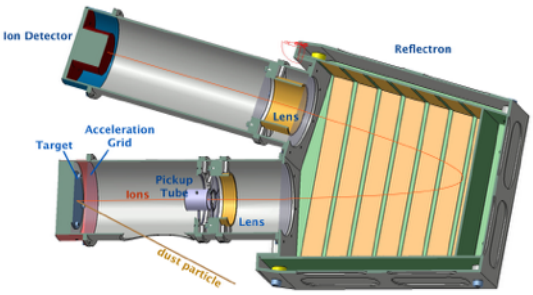

plasma charges. In the positive measurement mode electrons are collected at the iridium target plate whereas the cations are accelerated towards the reflectron drift tube. In negative mode, anions are accelerated. The reflectron corrects the ion energy distribution and increases the mass resolution. Depending on the density of the dust environment the sensitive area of the impact target can be switched between 0.8 cm^2 and 12,5 cm^2, respectively. The ions are collected at the ion detector where a mass spectrum is recorded. Up to 50 full spectra can be recorded per second, each spectrum representing the composition of an individual dust particle. The instrument is controlled by a radiation hardened FPGA and the instrument memory buffers 2048 complete spectra.

The High Flux Detector is a special operational mode with a continuous read-out of the induction channel 3 in order to derive gap-less stochastic impact statistics. Impact times are determined within 4 µs and ion yields are recorded for particle mass determination. This subsystem provides unique information about very high impact rates (up to 10^5 s^{-1}) and allows for accurate noise analysis.

A to-scale laboratory model of a ENIJA was built and tested at the dust accelerator in Heidelberg. Time-of-flight mass spectra were recorded using mineral and organic projectiles.

EPSC Abstracts
Vol. 10, EPSC2015-777, 2015
European Planetary Science Congress 2015

Re-evaluating Galileo Energetic Particle Detector data based on radiation detector decay; for use in estimating Sputtering Erosion rates on Europa.

Zoe Lee-Payne[1], Manuel Grande[1]. Norbert Krupp[2], Peter Kollmann[2, 3], Elias Roussos[2], Chris Paranicas[3]

1 – Aberystwyth University, UK
2 – Max Planck Institute for Solar System Research, Göttingen, Germany
3 - The Johns Hopkins University Applied Physics Laboratory, Maryland, USA

Abstract

The Energetic Particle Detector (EPD) launched in 1989 on the Galileo satellite took data on the Jovian Particle environment for 6 years before its demise [1]. Over the course of the mission the detectors in the Composition Measurement System (CMS) have visibly decayed with higher mass particles, specifically Oxygen and Sulphur, reading far lower energies at later epochs. By considering the non-steady accumulation of damage in the detector, as well as the operation of the priority channel data recording system in place on the EPD, an evolving correction can be made. Adjusting the data to account for the damage to the detectors will improve our understanding of the Jovian radiation environment. In particular, we can use the revised fluxes to re-evaluate the effect of the particle environment on the surfaces of the icy moons.

1. Introduction

This paper focuses on the PHA data from the EPD detector; specifically from the CMS telescope on the top of the instrument. The instrument uses foil films to detect time of flight of the incoming particle before they impact on the silicone semi-conductor detector at the end. This data has been analysed and can be displayed using ILD as a Pulse Height Analysis (PHA) graph as shown in Figure 2. The distinct loci visible in Figure 2 define the elements that were detected in the Jovian system, the uppermost is Sulphur followed by Oxygen, the faint line in the box labelled TA1 is Helium and the final loci is formed from Protons.

The loci of these elements reveal, when compared to those from near the end of the mission (Figure 2), that the detector is decaying in sensitivity. Figure 2 shows the same plot type from the 22nd October 2002, near the end of Galileo's mission. The same loci from Oxygen, Sulphur and Helium have all dropped in energy in varying amounts. The amount of energy drop corresponds to the element in question; as the dead layer of the semi-conductor detector thickens.

This thickening of the dead layer is the physical aspect of the decay and is caused by the radiation impacting onto the detector. This causes either the build-up of the silicone dead layer itself, or a build-up of sedimentation on the surface of the detector in addition to the dead layer. This affects only the energy readings of the composition measurements. The time of flight measurements stayed consistent during the mission; this makes the identification of element amounts in the Jovian plasma disk less accurate.

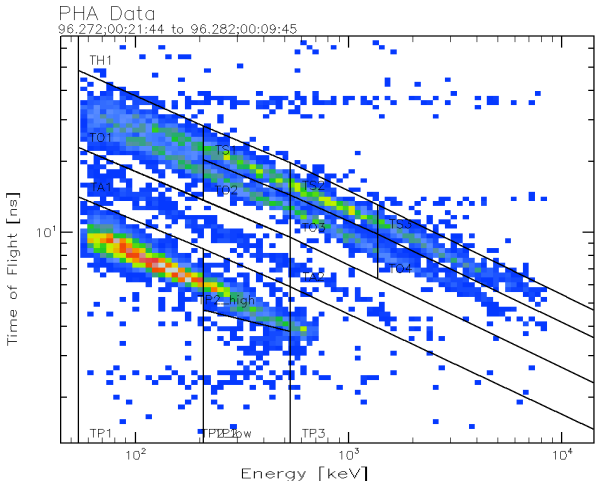

Figure 2: Pre-analysed EPD data beginning on the 29th Sep 1996 shortly after the arrival of Galileo in the Jovian system.

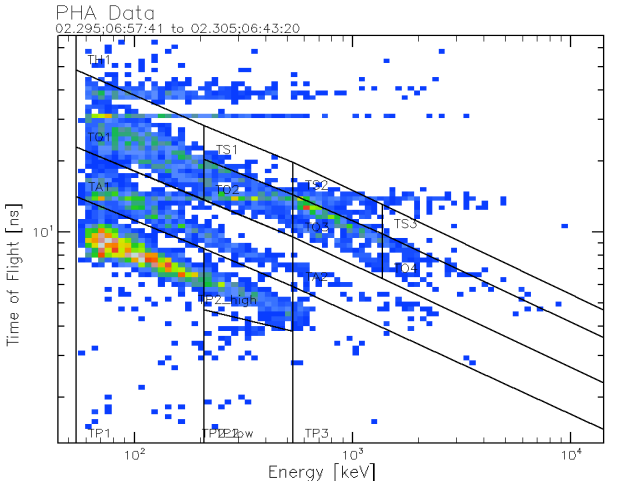

Figure 2:Pre-analysed EPD data beginning on the22nd Oct 2002 nearing the end of the mission lifetime shortly before the demise of Galileo into Jupiter itself.

There are many uses for having corrected data values for the radiation composition and energy levels in Jupiter's plasma disk. One of which is for analysing the effect of radiation on the surface of the Jovian moons. The corrected values will be the basis for sputtering calculations on the surface of Europa, updating the current estimates of the erosion rates as found in [2]. The new data could also be applied to current models, updating the estimates used in radiation analysis.

2. Correcting the data for radiation damage.

The data can be corrected by assuming a non-steady accumulation based on the position of the spacecraft and the time it has been in flight. By assigning a value to the amount of damage caused by a certain intensity of radiation incident on the detector, the value can be used to sum the decay based on the intensity and flight time.

The flight time of the spacecraft is important when the orbit path is observed in terms of an average intensity (Figure 4) (counts per second) incident on the detector (Figure 3). When plotted as intensity against the radius there is a clear distance from Jupiter which has far higher intensity than further out distances.

Europa's orbit is positioned at the peak R_J of the radiation intensity, $8R_J$. With the correction added to these values it can be seen how much the surface interactions can be changed.

For the data set available there are missing sections of data (Figure 4) for both intensity and position of spacecraft. These will have to be estimated to accurately compile the full amount of damage on the detector; even when there was

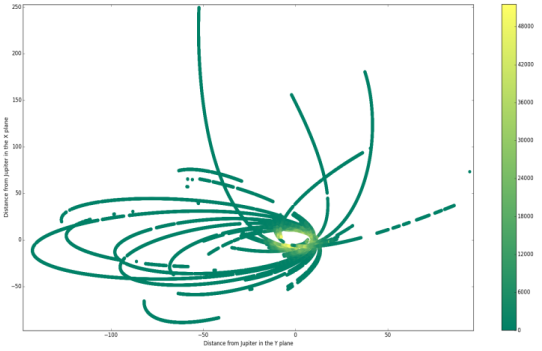

Figure 4: An orbit plot of Galileo's flight path around Jupiter. The colour bar signifies the CPS incident on the detector.

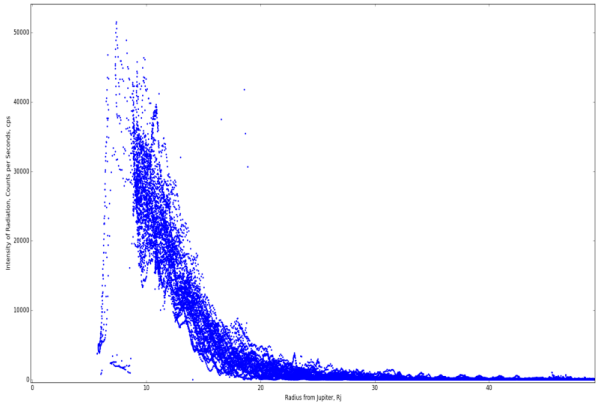

Figure 3: plot of the radiation intensity as a function of radius away from Jupiter in R_J. The intensity is plotted as counts per second incident on the detector.

no data being taken there would have still been particles hitting the detector. This is also true for the journey time to the Jovian system as well; there were recorded solar storms and flares that Galileo could have encountered on its journey that will have to be accounted for. This will most likely be a set value of damage that will carry some systematic error into the values, but that cannot be avoided.

3. Summary and Conclusion

The correction of the Galileo Jovian radiation data will be greatly useful in the areas of exploration, radiation analysis and also surface radiation interactions. The corrected values will allow far more detailed and accurate estimates to be made for the radiation erosion on Europa and on the other moons. It will also allow for better analysis of the surface composition of the moons, with the knowledge of what may have been artificially added to the surface from impacting and sputtered particles.

4. Acknowledgements

The authors would like to thank the EPD analysis team for the analysis software; written by Andreas Lagg.

5. References

[1] D. J. Williams, R. W. McEntire, S. Jaskulek, and B. Wilken, Space Science Reviews **60** (1-4), 385 (1992).

[2] C. Paranicas, B. H. Mauk, K. Khurana, I. Jun, H. Garrett, N. Krupp, and E. Roussos, Geophysical Research Letters **34** (15) (2007).

EPSC Abstracts
Vol. 10, EPSC2015-789-1, 2015
European Planetary Science Congress 2015

Thermal Radiometer Signal Processing using Radiation Hard CMOS Application Specific Integrated Circuits for use in Harsh Planetary Environments

G. Quilligan, J. DuMonthier, S. Aslam, B. Lakew, I. Kleyner, and R. Katz
NASA Goddard Space Flight Center, Greenbelt, MD 20771; gerard.t.quilligan@nasa.gov

Abstract

Thermal radiometers such as proposed for the Europa Clipper flyby mission [1] require low noise signal processing for thermal imaging with immunity to Total Ionizing Dose (TID) and Single Event Latchup (SEL). Described is a second generation Multi-Channel Digitizer (MCD2G) Application Specific Integrated Circuit (ASIC) that accurately digitizes up to 40 thermopile pixels with greater than 50 Mrad (Si) immunity TID and 174 MeV-cm^2/mg SEL. The MCD2G ASIC uses Radiation Hardened By Design (RHBD) techniques with a 180 nm CMOS process node.

1. Introduction

Thermopile pixels provide a linear voltage response to infrared wavelengths in the 7-200 µm range making them suitable for thermal radiometers. A radiometer sensor with a custom designed 2D array and eight ASICs arranged in a hybrid Focal Plane Assembly (FPA) is shown in Figure 1. The hybrid package size is 86.3 mm x 63.5 mm x 8 mm. This implementation has 5 line arrays on one substrate giving a total of 320 pixels. Each 64-pixel line array has a unique passband. The spectral passbands are 7-10 µm, 12.5–25 µm, 25-50 µm, 50-100 µm and 100-200 µm. The different passbands allow the measurement of endogenic heat flux, hotspot detection and day/night surface temperatures of an icy moon such as Europa. Sub-microvolt outputs from the pixels necessitate gains in the region of several thousand. The thermal noise of the pixel outputs and the 1/*f* noise [2] of the amplifiers must be filtered in order to achieve adequate signal to noise ratio before digitization. The thermopiles are operated at cryogenic temperatures so as to minimize thermal noise. The front-end electronics must also operate at temperatures as low as 150 K in the high TID environment present in the Jovian orbital system. Sampled analog signal processing is used in the custom ASIC to accurately amplify and digitize the outputs of thermopile pixels.

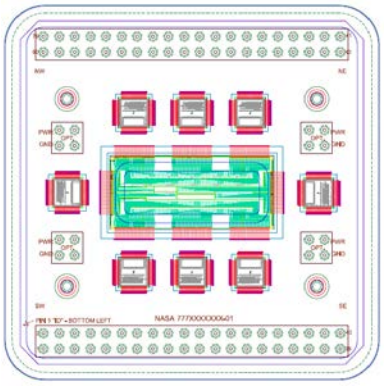

Figure 1: Radiometer focal plane assembly, showing the layout of thermopile line arrays and ASICs.

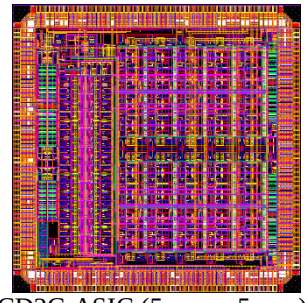

Figure 2: MCD2G ASIC (5 mm x 5 mm) will digitize up to 40 thermopile pixel voltage outputs.

2. Multi-Channel Digitizer

The MCD2G ASIC digitizes multiple thermopile pixels. It was built in a commercial 180 nm CMOS node using RHBD techniques to achieve TID/SEL immunity [3]. The first generation MCD ASIC digitizes up to 18 pixels while the second generation MCD2G accommodates up to 40 pixels, Figure 2. Figure 3 shows a block diagram for the MCD2G.

Each channel combines chopper stabilization with filtering to amplify the microvolt level signals from the thermopiles. A 16-bit Sigma-Delta Analog-Digital Converter (SDADC) then digitizes the resulting signals. The approximate channel gain is defined in the following equation (in the z-domain) where G is user programmable:

$$A_z \cong \frac{G}{1.05 - z^{-1}} \quad (1)$$

G can have the following values: 6.25, 12.5, 39, 156 and 625. The channel frequency response is plotted for G = 156 and T_{clk} = 4 µs in Figure 4. The channel outputs can also be averaged by the SDADCs. A plot of V_{out} vs V_{in} for one channel measured before-after 50 Mrad (Si) of TID is shown in Figure 5.

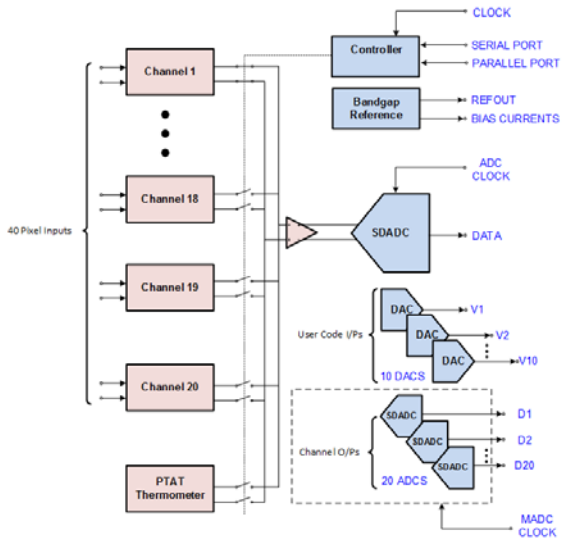

Figure 3: MCD2G block schematic.

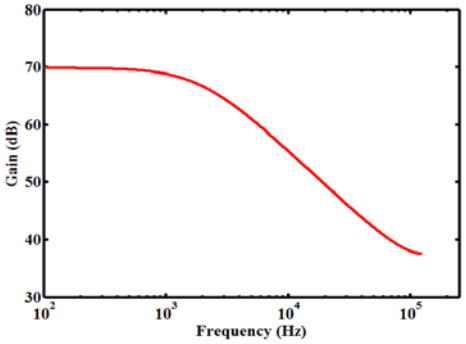

Figure 4: Channel Bode plot (G = 156, T_{clk} = 4 µs).

The ASIC measures its own junction temperature which, when in close proximity to the array, allows the user to calibrate the thermopile pixel measurements. It also provides ten general-purpose variable voltage outputs, which may be used for bias and control of the FPA. The ASIC's serial port allows the instrument designer to minimize cable mass with only several wires needed to control multiple ASICs. The ASIC also outputs all of its data through an LVDS signal pair.

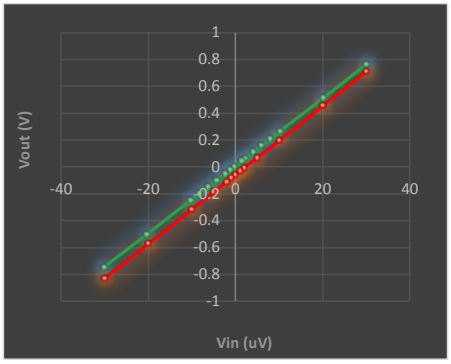

Figure 5: Gain before (green) and after (red) 50 Mrad (Si) gamma-ray TID.

3. Summary and Conclusions

A radiation hard multi-channel digitizer ASIC, built in a 180 nm commercial CMOS node, interfaces directly between a radiometer's thermopile line arrays and a digital controller with very high immunity to TID and SEL. The ASIC provides variable gains with filtering for 1/*f* and thermal noise.

Acknowledgements

Goddard Space Flight Center's IRAD program funded the MCD ASIC development in collaboration with Towerjazz Semiconductor, Newport Beach, CA.

References

[1] Europa Clipper Proposal Information Package: JPL D-92256, 2014.

[2] Hanel, R., Conrath, B., Jennings, D. and Samuelson, R.: Exploration of the Solar System by Infrared Remote Sensing 2nd Edition, Cambridge University Press, 2003.

[3] Quilligan, G., Aslam, S., and Lakew, B.: A 0.18 µm CMOS Thermopile Readout ASIC Immune to 50 Mrad (Si) Total Ionizing Dose and Single Event Latchup to 174 MeV-cm^2/mg, IWIPM 2014, 4-7 November 2014, Pasadena, California, USA, 2014.

EPSC Abstracts
Vol. 10, EPSC2015-813-2, 2015
European Planetary Science Congress 2015

Radiation and Dust Sensor for MARS2020: technical design and development status overview

V. Apéstigue (1), I. Arruego, J. Martínez, J.J. Jiménez, J. Rivas, M. González, J. Álvarez, J. Azcue, A. Martín-Ortega, J.R. de Mingo, M. T. Álvarez, L. Bastide, A. Carretero, A. Santiago, I. Martín, B. Martín, M.A. Alcacera, J. Manzano, T. Belenger, R. López, D. Escribano, P. Manzano, J. Boland (2), E. Cordoba (2), A. Sánchez-Lavega (3), S. Pérez (3), A. Sainz López (4), M. Lemmon (5), M. Smith(6), C. E. Newman (5), J. Gómez Elvira(1,4), N. Bridges (6), P. Conrad (7), M. de la Torre Juarez (2), R. Urqui (1,4), J.A. Rodríguez Manfredi(1,4).

(1) Instituto Nacional de Técnica Aeroespacial (INTA), Spain. (2) Jet Propulsion Laboratory (JPL), USA (3) Universidad Pais Vasco, Spain. (4) Consejo Superior de Investigaciones Científicas (CSIC), Spain (5) Ahsima Research, USA, (6) The John Hopkins University, USA, (7) Goddard Space Flight Center NASA, USA

Abstract

MEDA (Mars Environmental Dynamics Analyzer) is a payload to be included in the rover of the MARS2020, NASA mission. The RDS (Radiation and Dust Sensor) is part of this set of instruments and consists on a suite of photodetectors with different spectral bands and a dedicated CCD pointed to the sky. The main objective of the instrument is to characterize the Mars dust opacity, size and morphology. We report on the design and development of this sensor.

1. Background

MEDA RDS incorporates two main sensing technologies: a set of discrete photodetectors and a CCD. A large heritage exists for both of them from previous missions:

On the photodetectors side, heritage comes from:

- REMS-UV instrument on MSL. REMS (Rover Environmental Monitoring Station) [5] is one of the 10 scientific instruments on board MSL's Curiosity Rover.

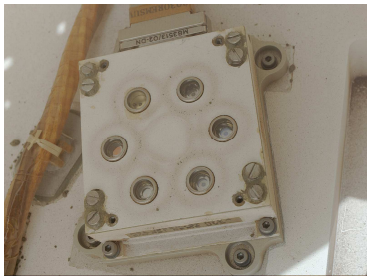

Figure 1: REMS UV Sensor.

REMS is a set of sensors aimed at the in-situ characterization of meteorological and atmospheric phenomena in the low atmosphere. It includes air and ground temperature sensors, wind sensors, humidity and pressure sensors, and also a reduced photometer focused on UV radiation. A mixed-signal ASIC designed for being able to operate in the Martian ambient temperature, outside thermally conditioned compartments, performs the main signal conditioning tasks. The UV [9] photometry is based on SiC detectors and interference filters.

- MetSIS [4] on Mars MetNet Lander [1]. The Photodetectors-based part of RDS, will mostly take advantage of the previous developments carried out in the frame of two different Mars explorations missions: Mars MetNet Lander and ExoMars 2016.

Figure 2: MetNet QM Penetrator and inflatable heat shielding.

Mars MetNet Lander is a tri-lateral mission developed by Russia, Finland and Spain, that aims to deploy a meteorological network (at a planetary scale)

on Mars surface. It will be based on penetrator-type landers that make use of inflatable devices for the Entry, Descent and Landing phase. As in any other mission, resources such as mass and power are extremely scarce. A compact "Solar Irradiance Sensor" (MetSIS) has been developed by INTA to be part of the meteorology payload of the first penetrator (MetNet Precursor). This MetSIS has been fully qualified for MetNet requirements, including low-temperature operation. It is designed as a single-box unit that includes 32 detecting elements in 11 spectral bands, distributed in 5 different orientations (zenith pointing detectors, plus lateral detectors sweeping 360º in azimuth). It also contains the conditioning front-end electronics, A/D conversion, control logic, internal memory and a digital serial I/F to a main computer. It allows autonomous and configurable operation (sampling rate, channels to be sampled, etc.). The sensing elements are composed of Si photodiodes and a combination of interference and density filters, plus FoV-shaping elements built in the structure

- DREAMS-SIS on ExoMars 2016: This mission includes a technology-demonstration of an Entry and Descent Module (EDM) that contains some short-life scientific payload. The main payload package is a meteorological sensor suite, called DREAMS [3]. DREAMS-SIS [14] is the photometer developed for this package and it makes use of the same design concepts and technologies used in MetSIS, although in this case it is composed of 2 separate units: Optical Head (OH) and Processing Electronics (PE). This is due to the special accommodation requirements imposed to the sensor. The OH mass was limited to less than 26 g, also with strong envelope volume constraints. It contains 7 detectors, one of them facing zenith and the other six, in 2 different spectral bands (UVA and NIR), lying on the faces of a tetrahedron, thus providing 360º azimuth vision.

Figure 3: DREAMS Mast QM.

With regard to the CCD heritage, it consists in the reuse and accommodation of one of JPL's engineering cameras already used in MER [6] and MSL: Hazcams.

Figure 4: HazCams on MSL.

The Camera (renamed as SkyCam), includes the focal plane module, with 1024x1024 effective sensor and the main electronics box. The optics of SkyCam will be designed ad-hoc for the present application, including a shadowing mask, at low zenith angles, and a neutral filter near to the lens center.

2. Instrument Design

2.1 RDS-DP: Discrete Photodetectors

The sensor consists of two different cofigurations for this technology:

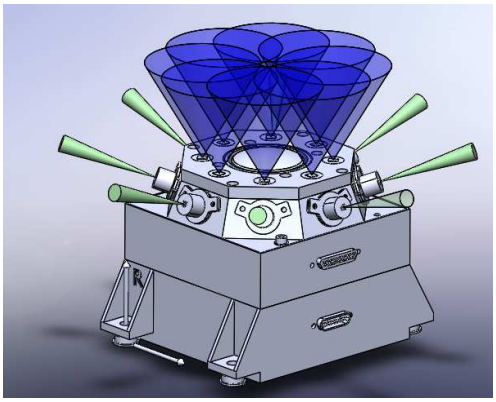

Figure 5: RDS-DP channels Field of View.

- Eight sky-view, narrow spectral channels that are pointing to the zenith. These channels will study the

aerosols opacity, occasional clouds and ozone column abundance. [9][14]

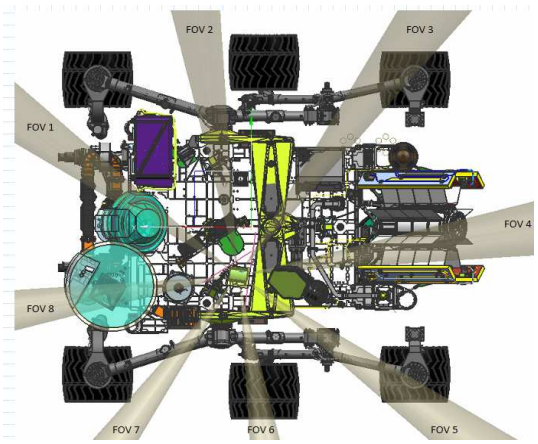

Figure 6: RDS rover accommodation.

- Eight 20º side pointing channels, separated 45º in azimuth, with the same wavelength, dedicated to measure the phase function to infer the shape and size of the dust.[2] [7][12][13].

The next tables summarizes the channels for the discrete photodetectors

Table 1: RDS-DP sky-view channels

DP Nº	Description	Wavelength (nm)	FoV (º)
1	O3 Redox	255 ± 5	± 5
2	O3	295 ± 5	± 5
3	UV	250-400	± 15
4	MZCAM cross cal.	450 ± 40	± 15
5	SkyCam cal.	650 ±25	± 15
6	MZCAM cross cal.	880 ± 5	± 15
7	Dust	950 ± 50	± 15
8	Phanchromatic	190-1000	± 90

Table 2: RDS-DP 20º side pointed channels

DP Nº	Description	Wavelength (nm)	FoV (º)
1-8	Sky brightness	880 ± 5	± 5

The detection range of the photodetectors is 190-1100nm due to its Si based technology. It is being considered to substitute three of them by a thermopile, with the aim to study the IR range up to 3µm (dust + ice clouds). This consideration depends on the results of the validation tests that are being developed for these sensors.

Each channel is configured as an opto-mechanical assembly [14]. The core of this set is the Si based detector (2 of figure 7) to provide the signal. An interference filter (3) is used encapsulated with the photodetector as a whole to discriminate each band. To obtain the corresponding FoV of the channel, a FoV-shaping element is placed (4). Then, the set is finished on top by a sapphire or a density filter (6) to enhance the optical response of the detectors and to avoid the dust deposition inside the drills of the FoV-shaping part. On the bottom, the opto-mechanical set is finished with a "radiation shield" (an aluminum plate) to complete a 1 mm radiation shielding protection of the box in any direction. The last part is a cobalt-samarium magnet ring (5) that prevents the dust deposition on the sensitive zone of the assembly (REMS heritage [5][9]).

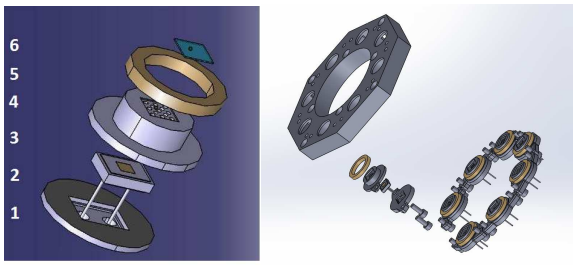

Figure 7: RDS-DP Opto-mechanical sets assembly.

RDS includes embedded electronics to perform the digital conversion of the different optical and handshaking channels. The core of the design will be and anti-fuse FPGA that be in charge of: acquire the different channels, handling/storage the digitalized data, and manage the communications with the MEDA Instrument Control Unit (ICU) by a master-slave protocol over RS422 differential interface. All this electronics will operate outside any warm box, with an operational temperature requirement going down to -130ºC.

2.2 RDS-SkyCam: CCD detector

A dedicated CCD element will be used to measure the dust opacity cycle and it size distribution. This sensor is intended to measure the intensity decay of the solar aureole [12] [13]

The SkyCam sensing element has a narrow spectral filter (880nm) and its optics has a neutral coating covering, near the noon solar angle (±15º from the lens center). This spectral band selection will allow to compare the intensity decay between the SkyCam signal and the 880 nm sky photodiode, when the sun reaches those high elevations.

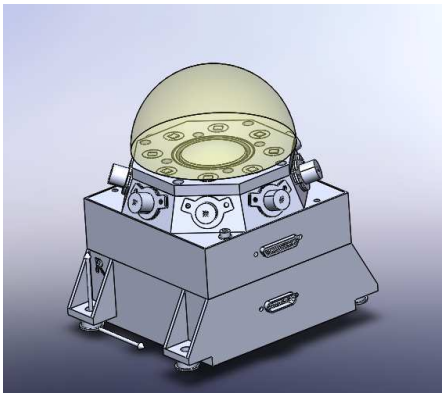

Figure 8: RDS-SkyCam.

3. Technology Validation Plan

One of the most demanding requirements in the design of instrumentation for Mars, is to survive to the extreme thermal cycling that the system will suffer during the mission. To prove that the technology used to manufacture the sensor is valid for the Mars surface, a particular test (PQV, Package Qualification and Verification) has been planned according to JPL/NASA requirements.

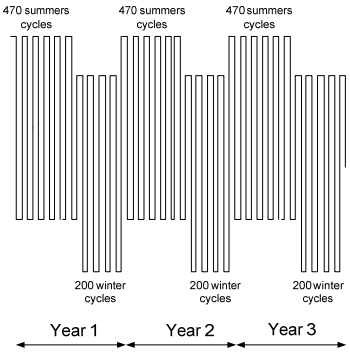

Figure 9: PQV Thermal Cycling Profile

This test tries to minimize the likelihood of packaging related failures (bonding, solder, etc.) at component level. At sub-assembly and unit level, it tests the mounting processes of all the used parts and materials. Figure 8, shows the thermal cycling profile of the test. It will simulate x3 mission time, with 1410 summer cycles from 40 to -105ºC at a maximum rate of 5º/min and 600 winter cycles from 15 to -130ºC at the same maximum rate.

The Validation Plan designed by INTA has been divided in two separate tests:

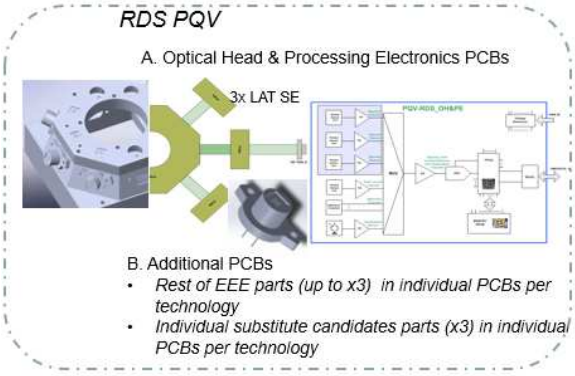

Figure 10: Technology Validation Plan for RDS.

A. Reduced version of RDS sensor: based on internal electronics used in previous Mars designs [4] [14], that have been thermally tested but with less than 2000 cycles. The design consists of two PCBs with all the necessary electronics to acquire 3 optical channels.

B. Additional PCBs: the rationale of this electronics boards is to test the same EEE Parts used in the previous option, in order to complete the quantity of 3 parts per part number tested. This approach will facilitate single tests to be performed on the components: visual inspections, X-ray, optical properties, etc. Identified parts substitutes, in case of components failure, have been incorporated also to this test PCBs.

Regarding the SkyCam, it has been tested according to MSL [11] requirements. Therefore, it can be used “as it is” for the RDS and does not need to be included in the validation plan.

4. Future Work

A dedicated PQV test is planned for thermopiles by the MEDA TIRS sensor team. Depending on the

behavior of this technology, it will be considered to be included on the RDS, substituting some sky-pointing Si-based photodetectors.

From that point and fordward, the design of the sensor will follow the usual path of any space payload: detailed design through CDR, qualification, calibration, etc., applying a model philosophy that will include engineering, qualification, flight and spare units.

4. Summary and Conclusions

The RDS sensor of MEDA package has been presented. This sensor will be the first one at Mars surface fully devoted to characterize the sun brightness and to provide a dedicated camera and low elevation, 360º azimuth coverage detectors, to study the dust conditions of the atmosphere. Its measurements will have a synergy on its investigations with previous mission sensors: REMS UV[9] and DREAMS SIS [14] and with sensors presents on the same rover: MastCAM-Z [10] and Sherloc [8].

In summary, MEDA RDS will be a very powerful tool to improve the knowledge of the Mars atmosphere and to enhance the radiative and atmospheric models of the red planet.

Acknowledgements

Part of this work has been funded with the help of the Spanish National Research, Development and Innovation Program, through the grant ESP2014-54256-C4-3-R.

References

[1] A.-M. Harri, W. Schmidt, H. Guerrero and L. Vázquez, Future Plans for MetNet Lander Mars Missions, European Geosciences Union General Assembly, 2014.

[2] Dubovik, O., and M.D. King, A flexible inversion algorithm for retrieval of aerosoloptical properties from Sun and sky radiance measurements, J. Geophys. Res., 105, D16, 2000.

[3] F. Esposito, et al., DREAMS for the ExoMars 2016 mission: a suite of sensorsfor the characterization of Martian environment, European Planetary Science Congress, 2013.

[4] H. Guerrero, Development of miniaturized instrumentation for Planetary Exploration and its application to the Mars MetNet Precursor Mission European Geosciences Union General Assembly, 2010.

[5] J. Gómez-Elvira et al., REMS: The Environmental Sensor Suite for the Mars Science Laboratory Rover, Space Science Review DOI 10.1007/s11214-012-9921-1, 2012.

[6] J. N. Maki , J. F. Bell III, K. E. Herkenhoff, S. W. Squyres, A. Kiely, M. Klimesh, M. Schwochert, T. Litwin, R. Willson, A. Johnson, M. Maimone, E. Baumgartner, A. Collins, M. Wadsworth, S. T. Elliot, A. Dingizian, D. Brown, E. C. Hagerott, L. Scherr, R. Deen, D. Alexander, and J. Lorre, Mars Exploration Rover Engineering Cameras, JOURNAL OF GEOPHYSICAL RESEARCH, VOL. 108, NO. E12, 807, 2003.

[7] Lemmon, M.T., M.J. Wolff, M.D. Smith, R.T. Clancy, D. Banfield, G.A. Landis, A. Ghosh, P.H.Smith, N. Spanovich, B. Whitney, P. Whelley, R. Greeley, S. Thompson, J.F. Bell III, and S.W. Squyres, Atmospheric Imaging Results from the Mars Exploration Rovers: Spirit and Opportunity, Science, 2004.

[8] L.W. Beegle, R. Bhartia, L. DeFlores, M. Darrach , R.D. Kidd, W. Abbey, S. Asher , A. Burton , S. Clegg, P.G. Conrad, K. Edgett, B. Ehlmann, F. Langenhorst, M. Fries, W. Hug, K. Nealson, J. Popp, P. Sobron, A. Steele, R. Wiens , K. Williford, SHERLOC: Scanning Habitable Environments with Raman and Luminescence for Organics & Chemicals, an investigation for 2020 International Workshop on Instrumentation for Planetary Missions (IPM), 2014.

[9] María-Paz Zorzano, Francisco Javier Martín-Torres, Rafael Navarro-Gonzalez, Javier Martín-Soler, Javier Gómez-Elvira, REMS Ultraviolet Sensor: First UV measurements from the Martian Surface, European Geosciences Union General Assembly, 2013.

[10] N. Maki, G.L. Mehall1, M.A. Ravine3, M.A. Caplinger and the Mastcam-Z Science Team, MASTCAM-Z: a Geologic, Stereoscopic, and Multiespectral Investigation on the NASA MARS-2020 ROVER. International Workshop on Instrumentation for Planetary Missions (IPM), 2014.

[11] Rajeshuni Ramesham, , Justin N. Maki, and Gordon C. Cucullu, Qualification Testing of Engineering Camera and Platinum Resistance Thermometer (PRT) Sensors for Mars Science Laboratory (MSL) Project under Extreme Temperatures to Assess Reliability and to Enhance Mission Assurance, International Society of Optics and Photonics (SPIE), 2008.

[12] Smith, M.D. and M.J. Wolff, Seasonal Variation of Aerosol Particle Size Using MER/Pancam Sky Imaging. AGU Fall Meeting, 2013.

[13] Smith, M.D., M.J. Wolff, R.T Clancy and S.L. Murchie (2009), Compact Reconnaissance Imaging Spectrometer Observations of Water Vapor and Carbon Dioxide, J. Geophys. Res., 114, 2008.

[14] V. Apéstigue, J.J. Jiménez, J. Martínez, F.J Álvarez, J. Rivas, M. González-Guerrero, J. Azcue, M.R Canchal, I. Martín, M. Álvarez, I. Arruego, DREAMS-SIS: A Miniature Instrument for the Measurement of Atmospheric Optical Depth on Exomars 2016 EDM, International Workshop on Instrumentation for Planetary Missions (IPM), 2016.

EPSC Abstracts
Vol. 10, EPSC2015-850, 2015
European Planetary Science Congress 2015

Solar Irradiance Sensor on the ExoMars 2016 Lander

I. Arruego, V. Apéstigue, J. Martínez, J.J. Jiménez, J. Rivas, M. González, J. Álvarez, J. Azcue, I. Martín, R. Canchal.

Instituto Nacional de Técnica Aeroespacial (INTA), Spain (arruegori@inta.es).

Abstract

DREAMS-SIS is a radiometer designed to provide in-situ measurements of the Sun irradiance on Mars surface, as well as to estimate the opacity of the Mars atmosphere, due to the suspended dust. It will be included in the DREAMS package (Dust characterization, Risk assessment and Environment Analyzer on the Martian Surface), payload of the EDM (Entry and Descend Module) for the EXOMARS 2016 ESA mission [1]. We report on the development and characteristics of this miniature sensor.

1. Introduction

DREAMS-SIS is a kind of evolution/simplification of a previous development (MetSIS), built for a different mission called Mars MetNet Lander [1]. The incorporation of this sensor to DREAMS was decided in an advanced stage of development of DREAMS and EDM. When it was done, the mass of MetSIS was not acceptable, given that the mast on top of which the sensor is lo be located, was not prepared to accommodate more than 25 g, with an extremely reduced volume envelope.

Due to that, a new SIS called DREAMS-SIS was developed. The unit was separated into 2 parts: Optical Head (OH) Processing electronics (PE), and the mechanical interfaces were defined so as to be adapted to the existing Mast. The OH contains the detectors and front-end conditioning electronics. The PE includes digital conversion, data handling/storage and communications capabilities with the DREAMS Central Electronics Unit (CEU). The OH will operate outside any warm box, with an operational temperature requirement going down to -120ºC.

The complete re-design, manufacturing, calibration and qualification, was done in only 10 months, due to system-level schedule requirements. 5 models have been manufactured (Engineering or EM, Qualification or QM, Flight or FM, Spare or SP and "Field-Test" for field campaigns, or FC).

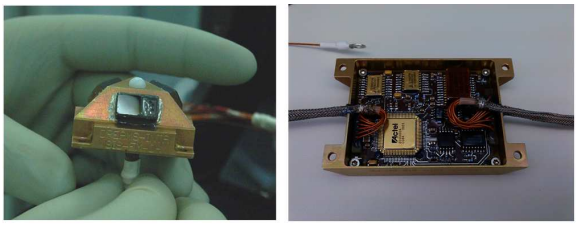

Figure 1. Left: Optical Head (OH). Right: Processing Electronics (PE)

2. Instrument design

The high level of integration of the sensor, and very specially the OH, was possible thanks to the use of commercial parts (COTS: Commercial Of The Shelf) previously selected, qualified (radiation and temperature) and screened thanks to the MetNet developments and an internal initiative for the development of miniature instruments developed during the past years, as described in [3].

2.1 Materials, Components and COTS selection.

DREAMS-SIS benefits from the previous work done mainly for MetNet, where an intensive radiation and extreme temperature qualification campaign was developed for different materials and parts.

As stated, especially for the OH some COTS had to be used, as no adequate space-grade parts are available for some of the functionalities, with the required mass and volume constraints. This applies to optoelectronic and optical parts, as well as the amplifiers used for the front-end electronics. All of them have been tested under Gamma radiation for TID, and protons for DD/SEE, depending on the kind of component.

Finally, those COTS have undergone adequate screening and qualification processes according to the next diagram (and following [4] to [7]):

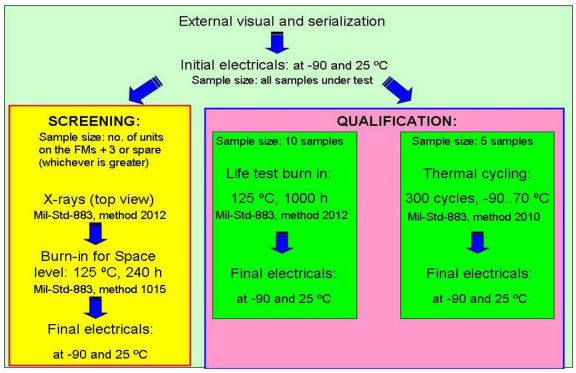

Figure 2. Flow diagram of the screening and reliability qualification processes adopted for Plastic COTS

2.2 Optical Head (OH) design

The adopted solution consists in a truncated tetrahedron with face inclination angles of 60º (to reduce the dust deposition on the sensors active area). On each "lateral" face there are 2 detectors with different optical filters (assembly 1 in Fig. 3). A seventh detector was added on top that includes no optical filter.

The 2 detectors of each "lateral" side (1.f) provide signal for the next bands: UVA (315-400nm) and NIR (700-1100nm). To discriminate these bands interference filters are used (1.d, 1.e). To avoid the widening of the spectral response of these filters at incidence angles superior than 30º, an opto-mechanical FoV-shaping element (sometimes referred to as "collimator") was added to correct the FoV of the photodiodes, on each lateral side (1.c).

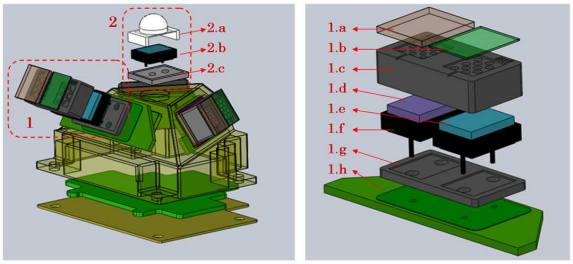

Figure 3. SIS OH Assembly. Opto-mechanical Set Assembly

The set is finished on top by two filters, an UG11 on the UV channel (1.a), and a transparent Teflon on the IR one (1.b), that were used to enhance the optical response of the detectors and to avoid the dust deposition inside the collimators.

On the other hand, the opto-mechanical set is finished on the bottom side (the one facing towards the inside of the OH box) with a "radiation shield" (an aluminum plate) to complete a 1 mm shielding protection of the box in any direction (element 1.g in Fig. 3). The whole assembly is attached to a PCB (1.h) that, on the bottom side, contains the signal amplifier electronics. To avoid electrostatic charging, the radiation shield and the collimators are later glued with a conductive glue (ECCOBOND 56C) to the OH structure.

The detector on top is a "total luminosity" Si detector (2.b) that incorporates no filter (i.e., its detection band is 200 – 1100 nm approximately) and is covered by a semi-spherical diffusing element (2.a) that helps minimizing the impact of the Sun position on the overall response and provides protection against dust deposition. On the bottom of the photodiode, another "radiation shield" was installed (2.c), again wired to the structure to avoid electrostatic charging.

The resultant geometry of SIS for DREAMS ensures that there will be measurements of both global and diffuse light contributions, with independence of the landing position. At almost any moment, one of the faces will be receiving direct plus diffuse light, whereas the others will only receive diffuse one.

SIS OH incorporates inside 4 different printed circuit boards (PCB). There is a main board located in the base of the OH that contains a multiplexer, power filter and buffering amplifier, to send the already-amplified photocurrent values to the PE. There is also a temperature sensor (platinum resistor) and a dark-current reference photodetector to measure the radiation accumulated (through Displacement Damage effect on the increase of dark current) during the flight to Mars. This main PCB also receives and conditions the photocurrent from the top detector (i.e. the total luminosity one). The multiplexer receives signals from the other 3 PCBs located on the lateral sides of OH. Connection between PCBs is done by means of wires.

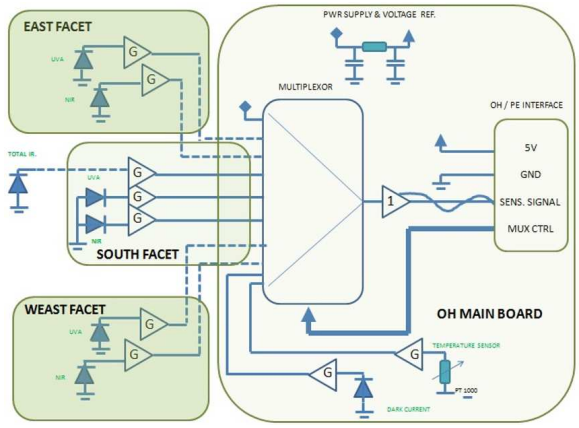

Figure 4. SIS OH Electronics diagram

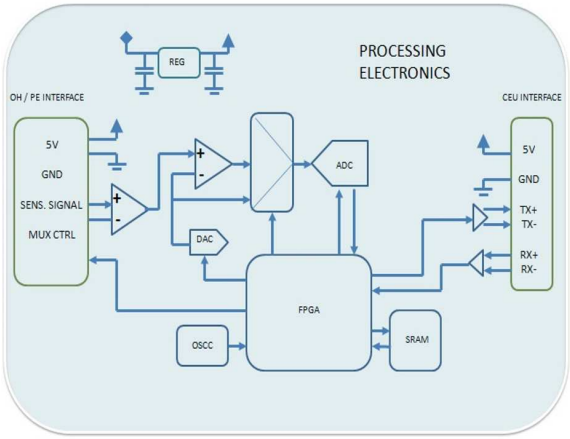

Figure 5. Fig. 1 SIS OH Electronics Schematics

Each one of these lateral PCBs contains the 2 aforementioned photodiodes and their corresponding transimpedance amplifiers that deliver voltage signals.

The interface with PE includes, as inputs, the 5V power supply and ground, received by means of a twisted pair, and 4 multiplexer selection lines received as single-ended signals (filtered at OH input). As out-puts, the OH delivers in a twisted pair the output signal from the multiplexer and its local ground, to allow for pseudo-differential reception on PE side.

2.3 Processing Electronics (PE) design

In this case the mechanical design is much simpler than OH's one. It has been designed in aluminum of 1mm thickness and it has no lid in order to be as light as possible. The CEU structure itself is used as lid.

The unit contains a unique PCB where the core is an ACTEL antifuse RTSX FPGA that controls the operation of the instrument: sequential acquisition of channels, averaging of multiple samples, calculation of standard deviation values, temporal storage on memory and communication with CEU.

PE receives the pre-amplified signals from OH with a differential amplifier. It receives only one signal from OH, which is the output of the OH multiplexer, whose active channel is selected by the PE FPGA, which controls the selection lines. Another multiplexer exists in the PE, to incorporate new housekeeping signals (PE temperature, power voltage and some voltage references).

The output of this PE multiplexer enters a subtraction and post-amplification scheme, prior to final digitalization, which allows a sub-ranging Analog-to-Digital (A/D) conversion. This means that, through a Digital-to-Analog (D/A) converter, the FPGA generates a voltage close to the value of the signal entering the post-amplifier, which is subtracted from the signal. After that subtraction, a new amplification takes place, and the A/D conversion is applied to the resulting signal. With this scheme we increase the dynamic range, while maintaining the linear response, in opposition to other classical logarithmic amplification solutions. The DAC being used to generate the subtracting signal has a resolution of 12-bit, although only the 6 MSBs are really used. The ADC is 16 bit.

A 128 bit Rad Tolerant SRAM memory is added to the system. It allows to perform some intermediate calculations (for example, to perform pseudo-noise estimation by computing a pseudo-sigma of a number of samples that are averaged). It also allows the sensor to operate in an autonomous mode, with no intervention of the CEU.

The basic operation mode is a "manual" one, in which CEU interrogates the sensor each and every time a new measurement is desired (which includes samples from all the channels). The aforementioned "automatic" mode, however, is an autonomous mode. At the beginning of an automatic session, the CEU just tells the instrument to go to this mode with a particular sampling period (configurable from seconds to minutes). When desired, the CEU commands the stop of the acquisition, and the internal memory can be dumped with a dedicated command.

3. Calibration

The method for the optical calibration of the SIS OH is based on the spectro-radiometric transfer from a standard lamp and a standard detector in well-controlled laboratory conditions.

The current generated by the photo-detector depends on its responsivity and on the incident optical power. Both parameters are a function of the wavelength and the relation is an integral. The responsivity depends on the temperature and also on the light incident angle, so the integral relation can be written:

$$I(T,\theta) = \int_0^\infty r(\lambda,T,\theta)E(\lambda)d\lambda \quad (1)$$

Where I(T,θ) is the current generated in the photo-detector and depends on the temperature and the light incident angle, r(λ,T,θ) is the spectral responsivity of the photodiode plus filters assembly. It depends on the wavelength, the temperature and the light incident angle. And E(λ) is the spectral incident light power.

In a first approximation, we can assume that the wavelength (λ), the temperature (T) and the light incident angle (θ) are independent variables. Then, we can write:

$$I(T,\theta) = r_T(T)r_\theta(\theta)\int_0^\infty r_\lambda(\lambda)E(\lambda)d\lambda \quad (2)$$

Where rθ(θ) is the Angular Response Function (ARF), rT(T) is Temperature Response Function (TRF) and rλ(λ) is the spectral responsivity under a perpendicular incident light at room temperature. We can write rλ as:

$$r_\lambda(\lambda) = R(\lambda_0)\cdot r'(\lambda) \quad (3)$$

Being r´(λ) the normalized responsivity with regard to a reference λ0, and R(λ0) a constant that represents the responsivity at λ0. Then, we can write:

$$I(T,\theta) = R(\lambda_0)\cdot TRF(T)\cdot ARF(\theta)\cdot\int_0^\infty r'(\lambda)E(\lambda)d\lambda \quad (4)$$

During the calibration process, E(λ) is known. r´(λ) is also known (after ad-hoc characterization done by the manufacturer and verified by INTA). We can solve the integral and get its value. This value (IE) is the amount of current generated in the hypothetical case that the detector had a responsivity of 1 at λ0. In this way, we can write:

$$I(T,\theta) = R(\lambda_0)\cdot TRF(T)\cdot ARF(\theta)\cdot I_E \quad (5)$$

This value (IE) depends on the optical channel, on the distribution of the input light spectrum and on the total incident optical power. The signal of a specific optical channel under the illumination of a specific spectral lamp with a determined light spectrum depends only on the incident optical power.

The TRF is defined to be equal to 1 at room temperature and the ARF is defined to be equal to 1 for a perpendicular light incidence. After these definitions, we can fix the temperature and the incident angle and we can change the optical power of the lamp. In this way, the experimental data can be fit in order to get the responsivity (R). Results for the FM model are shown in the next figure.

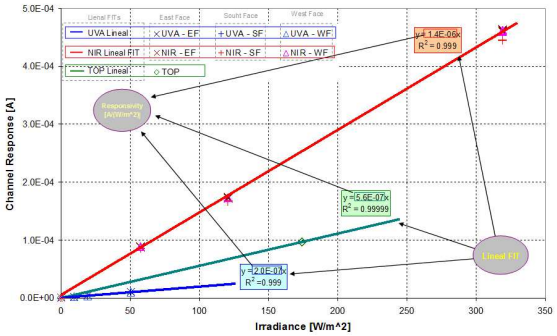

Figure 6. SIS FM responsivity calibration

Additionally, we can fix the optical power and the temperature and change the angle. In this way, we evaluate the ARF.

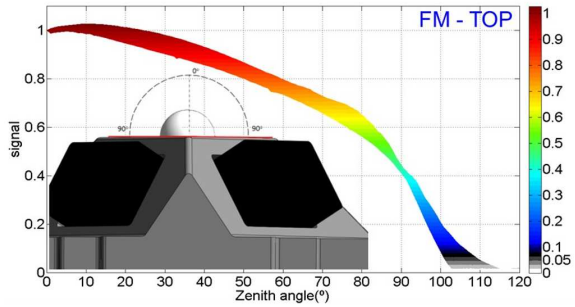

Figure 7. SIS FM "total light" (top) channel angular calibration

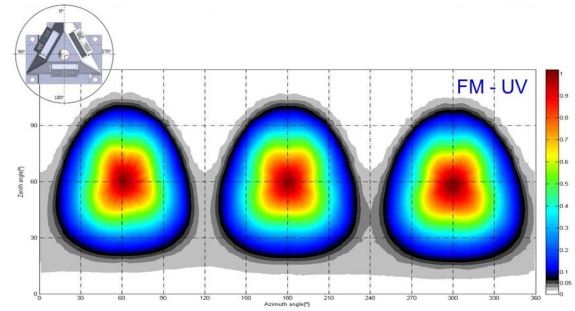

Figure 8. SIS FM UVA channels angular calibration

Finally, if we fix the optical power and the angle, we can get the TRF. In this case, we can calibrate the response of the temperature sensor as well. This was done in a vacuum chamber with optical window to allow excitation from the outside.

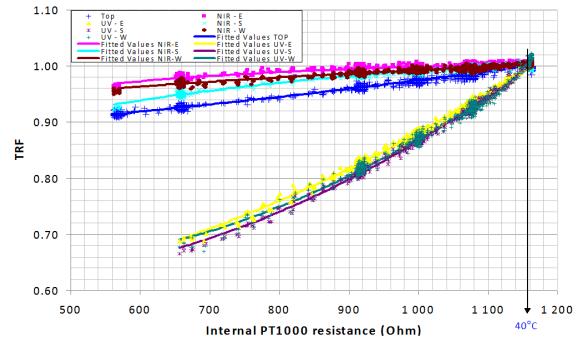

Figure 9. SIS OH FM thermal calibration

4. Qualification

The DREAMS SIS QM, FM and SPARE have passed the corresponding qualification and acceptance test levels according to the mission requirements. These test involve vibration (sine and random), thermal-vacuum, SRS shock and DHMR. For each model, optical characterization before and after the test campaign were done to verify the optical integrity of the instrument. Functional test and less intensive optical test were applied as well between tests (e.g., different axis of a vibration test) with the same aim.

All the assembly of the unit was done inside a laminar-flux cabinet in an ISO-6 facility, and observing Planetary Protection rules. The qualification campaigns were developed at corresponding INTA's facilities, but not always these facilities were compliant with the Planetary Protection requirements. In those cases, to avoid contamination of the units, special bagging procedures where applied to the transportation and for the test itself.

5. On-going activities

At present we are focused on the scientific retrieval algorithms. There are two main areas on which work is being developed:

5.1 Determination of Sun relative position

A priori it is not guaranteed that the Lander will provide information about its final attitude, once landed. The inclination of the horizontal plane on which the SIS lies, as well as its orientation within that plane, is of utmost importance in order to retrieve any information for which the relative position of the sun is relevant.

Due to this, during the last quarter of 2014 a big effort was done to qualify a miniature COTS accelerometer, accommodate it into SIS-PE box, and to acquire its signals at the expenses of removing some previously existing housekeeping signal. Only X and Y axis will be acquired. If the lander final inclination is moderate/high, with these signals we will recover the complete attitude information with a small error. In case it is small, the orientation of the sensor within the X-Y plane must be evaluated by other means.

We will do it by finding the time of the day for which the derivative of the signal provided by each detector is zero. This moment is related to the relative orientation of the Sun, and is found to show little dependence with the state (opacity) of the atmosphere. Next figure shows how the zero-value happens at the same moment regardless of the Optical Thickness (OT) value:

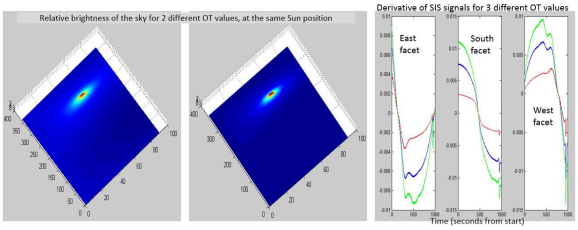

Figure 10. Left: Two different sky brightness models corresponding to 2 OT values. Right: Derivative of SIS signals for 3 different OT values from 0.1 to 2.2.

5.2 direct irradiance measurement and OT estimation

In July 2014 a measurement campaign was carried-out in a representative environment (Sahara Desert). An important set of reference instruments was carried to the dessert to be able to inter-compare their data with DREAMS-SIS: two pyranometers, one for measure the global irradiance and the second one to measure the integrated diffuse light (with a shadowing ring), one spectral-radiometer ASD-FS3 and one photometer CIMEL 318.

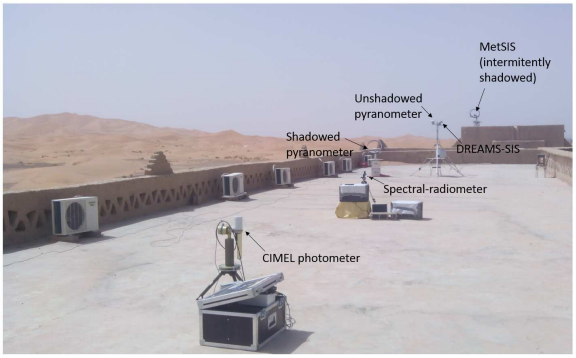

Figure 11. Image of the different instruments during the Sahara Desert campaign.

On one side, as shown in figure 12, the Sun irradiance value as recovered from SIS "Top" detector (hemispherical FoV, broadband: 200-1100 nm) is in very good agreement with the values provided by the pyranometers. The small differences (below 10% for Sun elevations above 40º) observed (Figure 12, bottom left) are due to the different angular responsivity of SIS and a pyranometer, which is uncorrected for the diffuse light.

On the other side, we estimate the OT value by doing as follows: (A) Compute the quotient between two signals of SIS (usually, the 2 biggest ones). (B) Simulate the sensor response for different sky brightness maps, corresponding to different OT's. (C) Calculate the same quotient from the simulations and identify the OT value that provides the closest result to the measured one. Radiation transfer models are needed for this.

In this way, SIS only makes use of relative measurements (quotient of 2 signals). If we assume, as per a random process, that the dust that will be deposited on each detector will produce approximately the same decrease of signal on each one, and giving that the measurement principle is fully differential, the degradation due to dust (or others, such as radiation) is negligible. At the same time, given that the measurements are simultaneous, we can obtain a "real time" estimation of the OT, instead of a daily average.

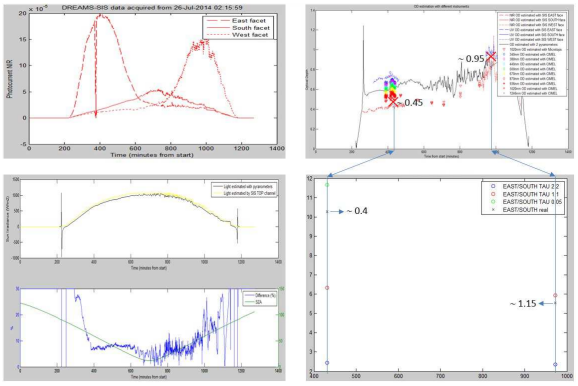

Figure 12. Left, top: real signals obtained from SIS in Sahara. Bottom: Sun irradiance calculated by SIS and pyranometer, and difference. Right, bottom: comparison of real signal quotients with simulated ones and identification of the estimated OT. Top: Measurements of OT for the same day and time, with different reference instruments.

6. Summary and Conclusions

The Solar irradiance Sensor on board the ExoMars 2016 Lander (as part of the DREAMS package) has been presented. It is a extremely miniaturized, low power and versatile (fully digital and autonomous) sensor, whose development was only possible thanks to the big effort done in qualification and screening of COTS parts.

It will allow obtaining direct Sun irradiance measurement and continuous OT estimation, with a full availability along the mission.

At present, the flight unit is already integrated in DREAMS, and being integrated in ExoMars Lander.

Acknowledgements

Part of this work has been funded with the help of the Spanish National Research, Development and Innovation Program, through the grant AYA2011-29967-C05-01.

References

[1] F. Esposito et al. (2014) 8th International Conference on Mars, #1246.

[2] A.-M. Harri et al. (2014) 8th International Conference on Mars, #1458.

[3] I. Arruego (2014) A Roadmap for the Development of Miniature Instrumentation for Mars Exploration. Second International Workshop on Instrumentation for Planetary Missions (IPM2014).

[4] MIL-STD-883H, method 2009.10, “External visual”.

[5] MIL-STD-883H, method 2012.8: "Radiography".

[6] MIL-STD-883H, method 1015.8: "Burn-in test".

[7] MIL-STD-883H, method 1010.8: "Temperature cycling".

EPSC Abstracts
Vol. 10, EPSC2015-891, 2015
European Planetary Science Congress 2015

Advanced Ion Mass Spectrometer for Giant Planet Ionospheres, Magnetospheres and Moons

E. Sittler (1), J. Cooper (1), N. Paschalidis (1), S. Jones (1), M. Rodriguez (1), A. Ali (2), M. Coplan (3), D. Chornay (2), S. Sturner (2), F. Bateman (4), N. Andre (5), A. Fedorov (5) and P. Wurz (6)
(1) NASA Goddard Space Flight Center, 8800 Greenbelt Road, Greenbelt, MD, 20771, (edward.c.sittler@nasa.gov / Fax: +1-301-286-1648), (2) University of Maryland, College Park, MD/NASA Goddard Space Flight Center, 8800 Greenbelt Road, Greenbelt, MD, 20771, (3) University of Maryland, College Park, MD USA, (4) National Institute of Technology and Standards, Gaithersburg, MD, USA, (5) IRAP, Centre National de la Recherche Scientifique, Toulouse, FR, (6) University of Bern, Physikalische Institut, Bern, Switzerland

Abstract

The Advanced Ion Composition Spectrometer (AIMS) has been under development from various NASA sources (NASA LWSID, NASA ASTID, NASA Goddard IRADs) to measure elemental, isotopic, and simple molecular composition abundances of 1 eV/e to 25 keV/e hot ions with wide field-of-view (FOV) in the 1 – 60 amu mass range at mass resolution $M/\Delta M \leqslant 60$ over a wide dynamic range of intensities and penetrating radiation background from the inner magnetospheres of Jupiter and Saturn to the outer magnetospheric boundary regions and the upstream solar wind. This instrument will work for both spinning spacecraft and 3-axis stabilized spacecraft with wide field-of-view capability in both cases. It will measure the ion velocity distribution functions (IVDF) for the individual ion species; ion velocity moments of the IVDF will give the fluid parameters (density, flow velocity and temperature) of the individual ion species. Outer planet mission applications are Io Observer, Jupiter Europa Orbiter/Europa Clipper, Enceladus Orbiter, and Uranus Orbiter as described in the decadal survey, but would also be valuable for inclusion on other missions to outer planet destinations such as Saturn-Titan and Neptune-Triton and for future missions to terrestrial planets, Venus and Mars, the Moon, asteroids, and comets, and of course for geospace applications to the Earth.

1. Introduction

The AIMS approach has a multi-mission capability in sub-systems can be removed or added in order to meet the planetary mission requirements. Emphasis is on Europa class mission due to its most demanding environment, since if this can be achieved one has the capability to do missions with less demanding environments. The least capable and lowest resource requirements with major ion detection emphasis but applicable, for example, to support magnetometer measurements of Europa's ocean, to the most capable higher resource option for which ion composition has the greatest emphasis with both major ion and minor ion detection capabilities along with wide dynamic range for measurements of the more tenuous magnetospheric plasmas to the denser plasmas within planetary ionospheres. The design of AIMS can be optimized for science operations in extreme radiation environments as would be encountered at Io and Europa, while also allowing full measurements in the more quiescent environments of the outer magnetospheric boundary regions and the upstream solar wind.

2. Summary and Conclusions

Our approach to increase signal to noise within the instrument is to 1) reduce foreground noise so scattering by major ions cannot hide the peaks of the minor ions by using our Circular Wien Filter (CWF) design with tophat electrostatic analyzer for wide field-of-view capability and 2) reduce background noise due to penetrating particles by reducing the effective area of the detectors without reducing geometric factor (GF) or sensitive area and then using sufficient shielding; reducing detector area allows shielding mass to be reduced. We have been measuring the response of microchannel plates to penetrating electrons from 100 keV to 1.5 MeV

electrons using the NASA Goddard Van de Graaff and 8 MeV to 27 MeV using the National Institute of Standards and Technology (NIST) linear accelerator with and without shielding. Other mitigating techniques can also be used. By combining the mass-per-charge (M/Q) selection capabilities of the CWF + ESA, and the Linear Electric Field (LEF) time-of-flight (TOF) sub-assembly, we can separate ions of similar M/Q like O+/S++ and O2+/S+; our LEF can use novel tapered design whose concept was originated by the Goddard AIMS group. Solid state detector is included for high charge state ion measurements. We also have the capability to detune the instrument's GF by > 1000. Laboratory measurements of the AIMS prototype instrument performance will be presented.

Acknowledgements

We would like to acknowledge the support we received from the Astrobiology Instrument Development (ASTID) program and support from the Goddard Chief Technologists Internal Research and Development (IRAD) Program.